Evidence of brain injury in fetuses of mothers with preterm labor with intact membranes and preterm prelabor rupture of membranes

Clara MURILLO M.D.[1,2], Elisenda EIXARCH M.D., Ph.D[1,2,3]*, Claudia RUEDA M.D.[1,2], Marta LARROYA M.D.[1,2], David BOADA M.D.[1], Laia GRAU M.D.[1], Júlia PONCE M.D.[1], Victoria ALDECOA[1], Elena MONTERDE M.D.[1,2], Silvia FERRERO M.D., Ph.D[1], Vicente ANDREU-FERNÁNDEZ Ph.D[2,4], Gemma ARCA M.D., PhD[1,2], Laura OLEAGA M.D., PhD [2,5], Olga ROS[1], Maria Pilar HERNÁNDEZ [5], Eduard GRATACÓS M.D., Ph.D[1,2,3], Montse PALACIO M.D., PhD[1,2,3]*, Teresa COBO M.D., Ph.D[1,2,3]*.

[1]BCNatal - Barcelona Center for Maternal-Fetal and Neonatal Medicine (Hospital Clinic de Barcelona and Hospital Sant Joan de Déu), Institut Clínic de Ginecología, Obstetrícia I Neonatología, Fetal i+D Fetal Medicine Research Center, Barcelona, Spain.

[2] Fundació de Recerca Clínica Barcelona - Institut d'Investigacions Biomèdiques August Pi I Sunyer (IIS-FRCB-IDIBAPS), Universitat de Barcelona. Barcelona, Spain.

[3] Center for Biomedical Research on Rare Diseases (CIBER-ER), Institute of Health Carlos III (ISCIII), 28029 Madrid, Spain.

[4] Biosanitary Research Institute, Valencian International University (VIU), 46002 Valencia, Spain.

[5] Radiology Department, CDIC, Hospital Clínic de Barcelona, Barcelona, Spain.

* These three authors contributed equally as last authors of the paper.

CONFLICT OF INTERESTS

The authors report no conflicts of interest.

FUNDING SOURCES

This study is funded by the competitive grant “Ajut a la recerca Josep Font” from Hospital Clinic from Barcelona. Clara Murillo was employed by the same grant “Ajut a la recerca Josep Font” for three years to carry out this project. Amniotic fluid analysis and costs for publication were also funded by the Institute of Health Carlos III (Proyectos de investigación en Salud, PI19/00580, PI22/00663). Elisenda Eixarch was partially supported by Convocatòria Intensificació Interna per als professionals de l’Hospital Clínic de Barcelona 2023, granted by the Hospital Clínic de Barcelona.

PAPER PRESENTATION INFORMATION

The findings of this paper were presented in the following meetings:

19th World Congress in Fetal Medicine. Fetal Medicine Foundation. Crete, Greece. 26-30th June 2022.

32nd World Congress 2022 on Ultrasound in Obstetrics and Gynecology. ISUOG. London, United Kingdom. 16-18th September 2023.

SMFM’s 43rd Annual Pregnancy Meeting. SMFM. San Francisco, California. 6-11th February 2023.

20th World Congress in Fetal Medicine. Fetal Medicine Foundation. Valencia, Spain. 25-29th June 2023

CORRESPONDING AUTHOR’S CONTACT INFORMATION: Eduard Gratacós.

gratacos@clinic.cat

WORD COUNT: Abstract: 423 words. Main text: 3575 Words.

TWEETABLE STATEMENT

Fetuses of mothers with preterm labor or preterm prelabor rupture of membranes have signs of brain remodeling and injury, as reported in infants and adults born preterm, suggesting these changes are, at least in part, already present prenatally.

SHORT VERSION OF TITLE:

Antenatal brain injury in fetuses presenting with preterm labor with intact membranes or preterm prelabor rupture of membranes.

AJOG AT A GLANCE:

A. Why was this study conducted? To evaluate the prenatal features of brain remodeling and injury associated with spontaneous preterm delivery and the potential influence of intra-amniotic inflammation.

B. What are the key findings? We found fetuses from mothers with preterm labor with intact membranes or preterm prelabor rupture of membranes had sonographic signs of brain remodeling, even in the absence of intra-amniotic inflammation. Thus, they had smaller cerebellum, lower corpus callosum area and decreased Sylvian fissure depth. Interestingly, these fetuses presented signs of brain injury with high concentrations of grey and white brain damage biomarkers such as amniotic fluid neuron-specific enolase; amniotic fluid protein S100B and amniotic fluid glial fibrillary acidic protein. All changes were particularly prominent in those exposed to intra-amniotic inflammation.

C. What does this study add to what is already known? This is the first study providing evidence of the existence of fetal brain remodeling and injury in fetuses from mothers with preterm labor with intact membranes or preterm prelabor rupture of membranes, and the causal role of intra-amniotic inflammation as a mediator of risk in these cases.

ABSTRACT

Background: Brain injury and poor neurodevelopment have consistently been reported in infants and adults born preterm. These changes occur at least in part prenatally and are associated with intra-amniotic inflammation. The pattern of brain changes has been partially documented by magnetic resonance imaging but not with neurosonography in combination with amniotic fluid brain injury biomarkers.

Objectives: To evaluate the prenatal features of brain remodeling and injury in fetuses from patients with preterm labor with intact membranes or preterm prelabor rupture of membranes and to investigate the potential influence of intra-amniotic inflammation as a mediator of risk.

Study Design: In this prospective cohort study, fetal brain remodeling and injury was evaluated by neurosonography and amniocentesis in singleton pregnant patients with preterm labor with intact membranes or preterm prelabor rupture of membranes between 24.0-34.0 weeks, with (n=41) and without (n=54) intra-amniotic inflammation. Controls for neurosonography were outpatient pregnant patients without preterm labor or preterm prelabor rupture of membranes matched 2:1 by gestational age at ultrasound. Amniotic fluid controls were patients with an amniocentesis performed for indications other than preterm labor or preterm prelabor rupture of membranes without brain or genetic defects whose amniotic fluid was collected in our biobank for research purposes matched by gestational age at amniocentesis.

The group with intra-amniotic inflammation included those with intra-amniotic infection (microbial invasion of the amniotic cavity and intra-amniotic inflammation) and those with sterile inflammation. Microbial invasion of the amniotic cavity was defined as a positive amniotic fluid culture and/or positive 16S ribosomal RNA gene. Inflammation was defined by amniotic fluid interleukin-6 >13.4 ng/ml in preterm labor and >1.43 ng/ml in preterm prelabor rupture of membranes. Neurosonography included the evaluation of brain structure biometric parameters and cortical development. As amniotic fluid brain injury biomarkers we selected neuron-specific enolase, protein S100B and glial fibrillary acidic protein. Data was adjusted for cephalic biometrics, fetal growth centile, fetal sex, non-cephalic presentation and preterm prelabor rupture of membranes at admission.

Results: Fetuses from mothers with preterm labor with intact membranes or preterm prelabor rupture of membranes had signs of brain remodeling and injury. First, they had a smaller cerebellum. Thus, in intra-amniotic inflammation, non- intra-amniotic inflammation and control groups, transcerebellar diameter (median (25^{th}; 75^{th} percentile)) was 32.7mm (29.8; 37.6), 35.3mm (31.2;39.6) and 35.0mm (31.3;38.3), respectively (p=0.019); vermian height was 16.9 mm (15.5 ;19.6), 17.2 mm (16.0;18.9) and 17.1mm (15.7;19.0), respectively (p=0.041).
Second, they presented a lower corpus callosum area (0.72mm^2 (0.59;0. 81), 0.71mm^2 (0.63;0.82) and 0.78mm^2 (0.71;0. 91), respectively (p=0.006).
Third, they showed a delayed cortical maturation (Sylvian fissure depth / biparietal diameter ratio was 0.14 (0.12;0.16), 0.14 (0.13;0.16) and 0.16 (0.15;0.17), respectively (p<0.001), and right parieto-occipital sulci depth ratio was 0.09 (0.07;0.12), 0.11 (0.09;0.14) and 0.11 (0.09;0.14), respectively (p=0.012)).
Finally, regarding amniotic fluid brain injury biomarkers, fetuses from mothers with preterm labor with intact membranes or preterm prelabor rupture of membranes, had higher concentrations of neuron-specific enolase (11804.6pg/ml (6213.4;21098.8), 8397.7 pg/ml (3682.1;17398.3) and 2393.7pg/ml (1717.1;3209.3), respectively (p<0.001)); protein S100B (2030.6 pg/ml (993;4883.5), 1070.3pg/ml (365.1-1463.2) and 74.8pg/ml (44.7;93.7), respectively (p<0.001)), and glial fibrillary acidic protein (1.01ng/ml (0.54;3.88), 0.965ng/ml (0.59;2.07) and 0.24mg/ml (0.20;0.28), respectively (p=0.002)).

Conclusion: Fetuses with preterm labor with intact membranes or preterm prelabor rupture of membranes had prenatal signs of brain remodeling and injury at the time of clinical presentation. These changes were more pronounced in those with intra-amniotic inflammation.

KEY WORDS: amniocentesis, biomarkers, cerebellum, corpus callosum, cortical maturation, fetal brain, glial fibrillary acidic protein (GFAP), intra-amniotic inflammation, microbial invasion of the amniotic cavity, neuron-specific enolase (NSE), neurosonography, preterm labor with intact membranes, preterm prelabor rupture of membranes, protein S100B, spontaneous preterm delivery.

MAIN TEXT

INTRODUCTION

Spontaneous preterm delivery is associated with brain injury and remodelling in the offspring. Children and adults born prematurely have increased incidence of cerebral palsy, impaired neurodevelopment, speech and audiovisual dysfunctions and psychiatric disorders, together with altered postnatal brain imaging, including changes in numerous relevant brain structures and cortical folding delay (lower gyrification index and cortical surface area compared to term controls, diffuse white matter gliosis, neuronal-axonal injury of the white and gray matter, periventricular leukomalacia and periventricular hemorrhagic infarction)[1-3]. Several lines of evidence support that brain injury in preterm infants occurred, at least in part, prenatally. First, children of mothers complicated with preterm labor (PTL) with intact membranes have poorer neurodevelopment regardless of whether delivery was preterm or not[4,5]. Second, magnetic resonance imaging (MRI) studies[6,7] in fetuses from pregnancies who later delivered preterm show a reduction in cortical and extra-cerebral spinal fluid volumes[6] and neuronal connectivity in the left-hemisphere pre-language region[7]. Third, amniotic fluid markers of brain injury, specifically neuron-specific enolase and protein S100B, are elevated in women with PTL[8,9]. Finally, intra-amniotic inflammation (IAI) is a risk factor for worse neurodevelopmental outcomes[10] and cerebral palsy at 3 years[11]. The role of IAI in the genesis of fetal brain damage is further supported by animal studies[12-16].

The pattern of prenatal brain injury in PTL and intact membranes and PPROM has been partially documented with MRI in two previous studies[6,7], but there are no studies evaluating fetal brain by ultrasound (US). Neurosonography allows a highly detailed evaluation and measurement of fetal brain structures and cortical development[17-19] and is more accessible to clinical setting than MRI. In addition, no previous studies have combined the use of fetal brain imaging with biomarkers of brain damage in the amniotic fluid. This could add further information to document prenatal brain injury and support the prognostic value of brain imaging changes and their relation with IAI.

In the present study, we aimed to comprehensively investigate the pattern of signs suggesting fetal brain injury and remodeling associated with spontaneous preterm delivery and their association with IAI. We prospectively evaluated neurosonography and amniotic fluid brain injury biomarkers in fetuses from pregnancies with PTL with intact membranes and PPROM, with and without IAI, and from uncomplicated pregnancies.

MATERIAL AND METHODS

Study design and population

This was an observational prospective cohort study including consecutive singleton pregnant patients complicated with PTL with intact membranes or PPROM between 23+0 to 34+0 weeks of gestation at BCNatal (Hospital Clínic and Hospital Sant Joan de Déu, Barcelona, Spain) from 2018 to 2021. As part of the local clinical protocol, patients with singleton pregnancies admitted with PTL with intact membranes or PPROM below 34 weeks were offered amniocentesis to rule in/out intra-amniotic inflammation. Eligible cases were patients who underwent amniocentesis at admission. A group of outpatient singleton pregnant patients not diagnosed with PTL with intact membranes or PPROM in the second and third trimester of pregnancy from US screening were also recruited as the control group, matched 2:1 by gestational age with the PTL with intact membranes or PPROM cases at study US.

Three groups of fetuses were compared: those of mothers admitted for PTL with intact membranes or PPROM with IAI (IAI group), fetuses with PTL with intact membranes or PPROM without IAI (non-IAI group), and the previously described control group.

We also performed a sub-analysis of the IAI group. Thus, the IAI group was divided according to the presence or absence of microbial invasion of the amniotic cavity to the subgroups with intra-amniotic infection (both present) and with sterile intra-amniotic inflammation (just IAI present).

Amniocentesis to rule out intra-amniotic inflammation was not performed in the control group because there was no clinical indication for this purpose. Instead, in order to compare amniotic fluid brain damage biomarkers, 20 amniotic fluid samples from our Clinic-IDIBAPS biobank collected for indications other than PTL with intact membranes or PPROM or brain or genetic pathology were selected (biobank amniotic fluid samples). These amniocenteses were performed in the second or third trimester of pregnancy.

Exclusion criteria

The exclusion criteria were delivery before fetal neurosonography, maternal age below 18 years, multiple gestations, clinical chorioamnionitis[20] at admission, major fetal structural malformations or chromosomal anomalies, or PTL with intact membranes or PPROM cases without amniocentesis at admission.

Definitions

PTL with intact membranes was defined as regular uterine contractions with a cervical length up to the 5th centile[21] by transvaginal US. All patients had intact membranes. We only evaluated cervical changes by digital examination on suspicion of imminent delivery. PPROM was diagnosed as leakage of amniotic fluid confirmed by positive alpha 1 microglobulin protein test.

Inflammation was defined by the presence of high levels of amniotic fluid IL-6 measured by the enzyme-linked immunoassay (Diasource ImmunoAssays, Louvain-la-Neuve, Belgium), being 1.43 ng/ml the cut-off for PPROM cases[22] and 13.4 ng/ml for PTL with intact membranes cases [23] as previously reported by our group. The minimum detectable level of IL-6 was 0.2 ng/mL. The coefficient of variation was of 6.23 for a mean concentration of 123.3 pg/mL and 5.18% for a mean concentration of 317.4 pg/mL.

Microbial invasion of the amniotic cavity was defined as a positive amniotic fluid culture for genital mycoplasma (Mycoplasma IST 2, bioMérieux for *Ureaplasma* spp. or *Mycoplasma hominis*), aerobic (Chocolate agar) and anaerobic bacteria (Schaedler agar for anaerobes and thioglycolate broth). It was also diagnosed based on specific polymerase chain reaction amplification of the 16S ribosomal RNA gene using the primers: 5'-AGA GTT TGA TCC TGG CTC AG-3' and 5'-GGA CTA CCA GGG TAT CTA AT at-3' followed by Sanger sequencing. Sequences were identified using the Blast algorithm in the National Center for Biotechnology Information database, with a minimum of 98% of sequence identity.

Gestational age (weeks) was calculated according to first trimester crown-rump length[24].

Clinical management of preterm labor/preterm prelabor rupture of membranes

Two intramuscular injections of betamethasone 12 mg given 24 hours apart were administered for fetal lung maturation until 34+6 weeks. If there was no clinical contraindication, tocolysis (nifedipine, atosiban) was administered during steroid administration. We only administered broad-spectrum antibiotics to patients with PPROM, amniotic fluid glucose concentrations < 5 mg/dL, with microorganisms identified by Gram staining, positive amniotic fluid cultures, intrapartum *group B streptococcus* prophylaxis and in patients with clinical chorioamnionitis. From 2018-2019, patients with high suspicion of microbial invasion of the amniotic cavity received parenteral ampicillin 1g/6h and gentamycin 80 mg/8h and a single dose of oral azithromycin 1 g. Beyond 2019, our local protocol substituted this antibiotic combination to parenteral ceftriaxone 1g/12h and ampicillin 2g/6h and oral clarithromycin 500 mg/8h. Antibiotic treatment was discontinued when amniotic fluid cultures were negative. In women diagnosed with microbial invasion of the amniotic cavity who remained pregnant after microbiological results, we individualized the antibiotic treatment according to the microorganism isolated until 7-10 days. We changed to parenteral piperacillin-tazobactam 4g/6h when clinical chorioamnionitis was suspected. Labor induction was considered only if clinical chorioamnionitis occurred or after 34 weeks in women with microbial invasion of the amniotic cavity.

Fetal ultrasound and neurosonography assessment

Vaginal and abdominal fetal US and neurosonography were performed in the first 24-72 hours after amniocentesis in the group with PTL with intact membranes or PPROM and at similar gestational age in the control group. US was performed using Voluson E10 Expert and Voluson S8 US devices equipped with a 5-9mHz transvaginal transducer (GE Medical Systems, Zipf, Australia). The measurements were performed by two experienced examiners (CM, EE) who were blinded to amniotic fluid IL-6 concentrations and culture results at the time the US was done.

The study US protocol included the assessment of estimated fetal weight[25], conventional feto-placental Doppler and complete two-dimensional neurosonography following a strict standardized methodology[17,18,26] and according to the protocol of our institution [27].

Cephalic biometrics included biparietal diameter (BPD), occipito-frontal diameter (OFD), head circumference and cephalic index (calculated dividing BPD by OFD x100). Brain structure measurements included transcerebellar diameter[28], cerebellar vermian measurements (antero-posterior diameter and height)[28], antero-posterior pontine diameter[29], insular depth ratio[30] (defined as insular depth/ BPD), right and left, anterior and posterior horns of lateral ventricles[26,31,32], third ventricle[33], fourth ventricle width and height[34], cavum of the septum pellucidum width[35], cisterna magna[31] and craniocortical and sinocortical subarachnoid width[36] These measurements are illustrated in Figure 1.

Regarding cortical development, depths of the Sylvian fissure and parieto-occipital, calcarine and cingulate sulcus were measured according to previous studies[30,37,38] . Sylvian fissure, and the parieto-occipital, calcarine and cingulate sulci were also evaluated and graded from 0 to 5 according to a previous publication by Pistorius[39] (Figure 1).

Assessment of the corpus callosum included maximum length and body thickness[40]. Midsagittal DICOM images were processed using an in-house Matlab tool[41] (2009; The MathWorks Inc., Natick, MA, USA) for total corpus callosum area and Witelson subdivision evaluation. The total corpus callosum area was delineated through cursor-guided free-hand traces as the region limited superiorly by the hyperechoic sulcus of the corpus callosum and inferiorly by the cavum septi pellucidi and cavum vergae. The corpus callosum was then automatically subdivided into the seven areas described by Witelson *et al.* [42], including the rostrum, genu, rostral body, anterior midbody, posterior mid-body, isthmus and splenium areas (Figure 2). The delineation was performed twice in each case and the mean value was used for further analyses.

Wiltelson regions represent white matter tracts coming from different brain regions. Thus, rostrum corresponds to the caudal/orbital prefrontal and the inferior premotor regions; genus corresponds to the prefrontal region; rostral body corresponds to the premotor and supplementary motor regions; anterior midbody corresponds to the motor region; posterior midbody corresponds to the somesthetic and posterior parietal region; isthmus corresponds to the superior temporal and posterior parietal regions; and splenium corresponds to the occipital and inferior temporal region.

Amniotic fluid brain injury biomarkers (Neuron-specific enolase, protein S100B and glial fibrillary acidic protein) using multiplex immunoassay (Luminex technology) analysis

A total of 500 µl of amniotic fluid was collected immediately after amniocentesis and frozen at -80ºC. All samples were thawed and immediately centrifuged at 16,000 x g for 4 minutes prior to use or dilution. Total protein concentrations were evaluated using the Pierce™ BCA Protein Assay Kit (Thermo Scientific™, ref: 23225) to estimate the appropriate dilution factor for the Luminex assays. Samples were analyzed in duplicate and diluted as follows: 1/1 and 1/2 for glial fibrillary acidic protein (GFAP) and with a 1/5 and 1/10 dilution factor for protein S100B and neuron-specific enolase (NSE).

The GFAP DuoSet assay (DY2594-05) was used to detect GFAP and the Magnetic Luminex® Human Discovery assay (LXSAHM-04) was employed to detect protein S100B and NSE. All the commercial kits were manufactured by R&D systems™. This technology is based on magnetic bead sets labeled with specific concentrations of fluorescent dyes, resulting in more than 300 differentiated colored bead sets. The bead mixture is then incubated with the samples and the median fluorescence intensities are detected on a Luminex device. The LX100 (LX10010187403) device and XPonent software were used for 96-well MagPlex analyses with a minimum threshold of 50 events. Seven standards with a 1/3-dilution factor were used to perform the calibration curve from a stock solution of 13270 pg/mL for protein S100B, 90990 pg/mL for NSE and 20 ng/mL for GFAP. The lower limit of GFAP detection was 0.3 ng/ml. All the procedures were performed following the manufacturer's instructions.

Statistical analysis

Encoded information was processed by an Access database. Qualitative variables were described in tables as absolute frequency and relative percentage and quantitative variables as median and interquartile range (25^{th} centile-75^{th} centile).

The Shapiro Wilk test was initially used to assess continuous data for normality. For the baseline fetal, perinatal and admission characteristics of the study population, univariate analysis was performed using the Chi-square or Fisher's exact test for comparison of qualitative

variables. For quantitative variables, the Student's T-test was used for independent samples assuming a normal distribution except for the sub-analysis within the group exposed to IAI (microbial invasion of the amniotic cavity versus “sterile” inflammation), for which a non-parametric test was applied (Mann-Whitney U test). In this last sub-analysis, normal distribution was evaluated by the Shapiro-Wilk test and homoskedasticity by the Levene test. Wilcoxon-W test was applied for variables with a non-normal distribution.

Regarding sonographic and amniotic fluid biomarker analysis, multivariate analysis was performed using multiple linear regression (continuous variables) or logistic regression (categorical variables) controlling for possible confounding factors, which were: cephalic biometrics, fetal sex, fetal weight centile, non-cephalic presentation and PPROM at admission for the US evaluation; and fetal weight centile, fetal sex, gestational age at amniocentesis, and PPROM at admission for the amniotic fluid biomarkers. A linearity trend analysis was also performed in the three groups.

Finally, we performed Pearson’s correlation to evaluate the correlation between amniotic fluid IL-6 concentrations and brain structures among groups.

The data were analyzed by STATA for MAC (version 15.1 StataCorp LP). For the statistical analysis, p values ≤ 0.05 were considered as statistically significant.

Ethics

The Research Ethics Committees of the Hospital Clinic and Sant Joan de Déu reviewed and approved the study (HCB/2018/0567 and PIC 150-19, respectively) and all participants were informed and provided signed written consent.

RESULTS:

During the study period (2018-2021), 154 patients were admitted with a diagnosis of PTL with intact membranes or PPROM below 34 weeks. Among these, 116 were eligible for the study and 95 were finally included (Figure 3). Approximately 80% of the patients with PTL with intact membranes or PPROM had previously been included in other non-interventional studies[43,44].

Of the overall population, 34 patients had PPROM, 61 PTL with intact membranes and 48 were controls. Among the patients with PPROM and PTL with intact membranes, 41 had IAI (28/41 and 13/41, respectively). There were no differences in maternal characteristics (Table 1). All patients with microbial invasion of the amniotic cavity had intra-amniotic inflammation.

Table 2 shows clinical, ultrasound and biochemical comparison according to the presence of IAI in PTL with intact membranes or PPROM groups. Twenty percent of the total amniotic fluid cultures/16S rRNA were positive and the microorganisms isolated are shown in Table S1. Antenatal corticosteroids were administered in 100% of patients with PTL with intact membranes or PPROM and in 0% of the control group. Thus, adjustment for this parameter was not required. Fifty-seven percent of the patients diagnosed with PTL with intact membranes finally delivered at term.

Regarding fetal US, gestational age at US were similar among groups. However, we found a lower estimated fetal weight centile and a higher percentage of fetuses under the 10th centile in the IAI group without fetal-placental Doppler differences (Table 3).

Table S2 shows the gestational age and the indication for amniocentesis in the Biobank group selected to compare amniotic fluid biomarkers. All the genetic and infectious studies performed in these samples were normal and healthy offspring were confirmed in all cases.

Fetal brain in fetuses with intra-amniotic inflammation

Fetuses with IAI presented a lower transcerebellar diameter and cerebellar vermian height, while the insular depth ratio and fourth ventricular width were higher on comparison with the control group (Table 3).

Regarding cortical development, Sylvian and right parieto-occipital depth ratios were lower than controls (Table 4).

Corpus callosum total area and Witelson subregions 3, 5 and 6 (rostral body, posterior midbody and isthmus areas) were smaller (Table 4, Figure 4) than those of the control group.

Amniotic fluid NSE and protein S100B concentrations were significantly higher in the IAI group. GFAP was detected in 68.3% of fetuses with IAI and in only 30% of the control group (Table 5, Figure 5).

Sub-analysis: intra-amniotic infection vs. sterile intra-amniotic inflammation

Fetuses with sterile intra-amniotic inflammation had similar perinatal outcomes than those with intra-amniotic infection (Tables S4-S5). Only an enlarged cisterna magna and higher amniotic fluid protein S100B concentrations were observed in fetuses with intra-amniotic infection (Table S5-S6).

Fetal brain in the non-intra-amniotic inflammation group

Fetuses in the non-IAI group presented similar but less pronounced changes than IAI group regarding Sylvian fissure, corpus callosum total area and Witelson subregions and amniotic fluid protein S100B, NSE and GFAP (Table 4-5, Figures 3-4)

Correlation of amniotic fluid interleukin-6 concentrations with neurological changes

There was a significant correlation between amniotic fluid IL-6 concentrations and cerebral structures. Thus, higher amniotic fluid IL-6 concentrations were related to lower transcerebellar diameter, right parieto-occipital and right cingulate sulci depth ratio, total corpus callosum area,

Witelson subregions 3,6 and 7 and higher concentrations of amniotic fluid NSE and GFAP (Table S8).

COMMENT

Principal findings

Fetuses of mothers diagnosed with PTL with intact membranes or PPROM presented structural brain changes and signs of brain injury measured by neurosonography and amniotic fluid biomarkers. Although majority of changes were more pronounced in pregnancies with IAI, those without IAI also presented some differences with respect to controls, suggesting that IAI is a mediator but not the only factor associated with fetal brain injury in patients with PTL with intact membranes or PPROM.

Results in the context of what is known.

Our brain imaging findings are in line with previous MRI studies with smaller sample sizes [6,7] reporting prenatal brain changes in fetuses with a subsequent preterm delivery. The present study adds to previous knowledge by providing a comprehensive evaluation of fetal brain changes by neurosonography and evaluates additional brain structures than those previously reported. Another value of our study is the evaluation of cases according to the presence of absence of IAI, which provides an additional line of evidence to support the contribution of infectious/inflammatory status as a mediator of fetal brain injury associated with spontaneous preterm delivery.

Among the main fetal brain findings in this study, we found a smaller cerebellum in the IAI group, but not in the non-IAI group, when compared with controls. These findings are in line with a previous study in very premature infants and adolescents[2]. On the contrary, other authors[6] did not find changes on cerebellar volume prenatally, maybe because MRI was performed at an earlier gestational age than in the present study. Cerebellar growth is most prominent beyond 28 weeks[45,46]. Cerebellar damage in premature infants[2] has been related to worse cognitive outcome and motor disabilities [47-49].

In addition, fetuses with PTL with intact membranes or PPROM presented decreased Sylvian fissure depth and a larger insula, suggesting delayed cortical maturation. This finding has been previously reported in premature infants[50,51]. Changes were more pronounced in fetuses with IAI, which is in line with findings from animal models exposed to intra-amniotic

lipopolysaccharide (LPS) infusion[52]. Cortical sulci development has been associated to worse neurodevelopmental outcome[53], autism, and mood and speech disorders[54,55].

Finally, corpus callosum of fetuses with PTL with intact membranes or PPROM were smaller than controls with preservation of length but a reduction in the area of the medium and posterior regions. We hypothesize that this might be explained because corpus callosum length increases earlier in pregnancy, before the PTL with intact membranes or PPROM appear, while corpus callosum thickness increases following an anterior-to-posterior direction in the third trimester of gestation[56-58]. The results are in line with previous findings in premature infants[3] and in LPS-exposed fetal sheep [59]. Structural alterations of the corpus callosum are a predictor of impaired neurodevelopment and have been associated to worse speech outcomes neurobehavioral performance in adolescents and infants born preterm[60,61].

We found a significant correlation between amniotic fluid IL-6 concentrations and cerebellum, sulci depths, Witelson subdivisions and amniotic fluid concentrations of NSE and GFAP, which supports a mediating role of IAI in the genesis of brain injury and is in line with previous studies reporting that fetuses with IAI present worse postnatal results[10].

Regarding fetal brain damage biomarkers, increased concentrations of amniotic fluid protein S100B has been described before in patients with PTL with intact membranes and PPROM, with higher concentrations in those with IAI, in line with the present study. Postnatally, higher concentrations of serum and urine S100B have been related to schizophrenia[62], hypoxic-ischemic encephalopathy[63] and intra-ventricular hemorrhage[64]. Over-expression of serum NSE and S100B can predict neurodevelopmental adverse outcome at 1 year of life after cardiac arrest[65]. High concentrations of amniotic fluid NSE have been associated with postnatal gray matter injury, intraventricular hemorrhage, and periventricular leukomalacia in patients with PTL with intact membranes and subsequent preterm delivery[8]. Postnatally, high concentrations of NSE in cerebrospinal fluid has been correlated with worse neurodevelopmental outcomes at 2 years of life in arterial ischemic stroke and hypoxic-ischemic encefalopahy[66,67]. Higher concentrations on amniotic fluid GFAP have been related to neural tube defects[68] and higher

serum concentrations are considered a neuroinflammation biomarker in other conditions, such as multiple sclerosis [69].

Clinical implications

Prenatal brain changes seem to contribute to brain changes widely reported in preterm children and adults. Thus, our findings highlight the importance to early (prenatal) identify fetuses that will present postnatal neurological impairment, allowing the targeting of a high-risk population and the performance of preventive actions in the first months/years of life (including fetal life), when neuronal plasticity is maximum. The amniocentesis performed to rule in/out IAI helped to target the highest risk group of neonates that merits further follow-up.

Future research

Future studies are needed to assess postnatal changes in these cohorts of patients and identify possible prenatal predictors for neurological impairment. Prenatal neurological risk evaluation could be tremendously important, given the neurodevelopmental disorders reported in this population and the importance of early neurological stimulation or prenatal therapies to improve outcomes.

Strengths and limitations

The main strengths of this study are the prospective design and the recruitment of a well-characterized cohort of patients with PTL with intact membranes and/or PPROM with information on IAI, being the first cohort published with a complete fetal brain evaluation including both neurosonography and brain damage amniotic fluid biomarkers. Another strength is that the amniotic fluid brain damage biomarkers found in the control samples were concordant with those reported in previous studies [9,70]. Although MRI is considered a gold standard technique for brain evaluation, neurosonography has shown to be an adequate method to evaluate brain structures[17-19] and has demonstrated to be sensitive to show prenatal brain changes in placental disease[71,72], congenital heart disease[73], ventriculomegaly[74] and reproductive assistance techniques[75]. In comparison to MRI, neurosonography is more

accessible in the clinical setting, rapid to perform, cheaper and is not affected by issues related to the patient such as claustrophobe.

However, we also acknowledge some limitations. We excluded cases with imminent delivery without fetal neurosonography, as well as cases with anhydramnios without amniocentesis due to technical limitations. It remains unknown whether these patients might have a different profile than that of those studied. In addition, we acknowledge the lack of molecular techniques to diagnose IAI as another limitation. Indeed, it is possible that some of these patients may have a positive culture for fungi or viruses and were not detected. Another limitation was the lack of a clear and universal definition of intra-amniotic inflammation. In our study inflammation was defined according to amniotic fluid IL-6 concentrations but other authors include others inflammatory biomarkers[76,77]. We also acknowledge that only 69% of the patients with PTL with intact membranes or PPROM had an optimal corpus callosum image to assess the areas. Oligohydramnios, fetal position, and limited vaginal examination in patients with PTL with intact membranes and PPROM, due to the high risk of spontaneous preterm delivery in this group, were main determinants of the lack of assessment of these areas.

Finally, we acknowledge as limitation that a postnatal follow-up was not included. Further research is warranted to prospectively evaluate neurological changes postnatally in these cohorts before changing our clinical management in these patients.

Conclusions

Our findings suggest that structural brain changes including smaller cerebellum, corpus callosum medium-posterior areas and impaired cortical development in premature infants and adults might already be present in fetal life, at the time that symptoms of PTL with intact membranes and/or PPROM occur, especially in those with IAI. The observation of elevated concentrations of amniotic fluid NSE, protein S100B and GFAP strengthen our neurosonographic findings and support the hypothesis of the presence of prenatal brain injury in fetuses with PTL with intact membranes or PPROM, regardless to be born preterm or at term and the exposition to IAI.

FIGURES

TABLES

SUPPLEMENTARY TABLES

TABLE S8 Correlation between amniotic fluid IL-6 and brain structures and amniotic fluid biomarkers in preterm labor and preterm prelabor rupture of membranes groups

REFERENCES

1. Engelhardt E, Inder TE, Alexopoulos D, et al. Regional impairments of cortical folding in premature infants. Ann Neurol. 2015;77(1):154-162. doi:10.1002/ana.24313
2. Hinojosa-Rodríguez M, Harmony T, Carrillo-Prado C, et al. Clinical neuroimaging in the preterm infant: Diagnosis and prognosis. Neuroimage Clin. 2017;16:355-368. Published 2017 Aug 14. doi:10.1016/j.nicl.2017.08.015
3. Hart AR, Whitby EW, Griffiths PD, Smith MF. Magnetic resonance imaging and developmental outcome following preterm birth: review of current evidence. Dev Med Child Neurol. 2008;50(9):655-663. doi:10.1111/j.1469-8749.2008.03050.
4. Paules C, Pueyo V, Martí E, et al. Threatened preterm labor is a risk factor for impaired cognitive development in early childhood. Am J Obstet Gynecol. 2017;216(2):157.e1-157.e7. doi:10.1016/j.ajog.2016.10.022
5. Campos-Berga L, Moreno-Giménez A, Sahuquillo-Leal R, et al. Emotional regulation and psychomotor development after threatening preterm labor: a prospective study. Eur Child Adolesc Psychiatry. 2022;31(3):473-481. doi:10.1007/s00787-021-01733-6
6. Story L, Davidson A, Patkee P, et al. Brain volumetry in fetuses that deliver very preterm: An MRI pilot study. Neuroimage Clin. 2021;30:102650. doi:10.1016/j.nicl.2021.102650
7. Thomason ME, Scheinost D, Manning JH, et al. Weak functional connectivity in the human fetal brain prior to preterm birth. Sci Rep. 2017;7:39286. Published 2017 Jan 9. doi:10.1038/srep39286
8. Elimian A, Figueroa R, Verma U, Visintainer P, Sehgal PB, Tejani N. Amniotic fluid neuron-specific enolase: a role in predicting neonatal neurologic injury?. Obstet Gynecol. 1998;92(4 Pt 1):546-550. doi:10.1016/s0029-7844(98)00273-7
9. Friel LA, Romero R, Edwin S, et al. The calcium binding protein, S100B, is increased in the amniotic fluid of women with intra-amniotic infection/inflammation and preterm labor with intact or ruptured membranes. J Perinat Med. 2007;35(5):385-393. doi:10.1515/JPM.2007.101

10. Rodríguez-Trujillo A, Ríos J, Ángeles MA, et al. Influence of perinatal inflammation on the neurodevelopmental outcome of premature infants. J Matern Fetal Neonatal Med. 2019;32(7):1069-1077. doi:10.1080/14767058.2017.1399118
11. Yoon BH, Romero R, Park JS, et al. Fetal exposure to an intra-amniotic inflammation and the development of cerebral palsy at the age of three years. Am J Obstet Gynecol. 2000;182(3):675-681. doi:10.1067/mob.2000.104207
12. Polglase GR, Nitsos I, Baburamani AA, et al. Inflammation in utero exacerbates ventilation-induced brain injury in preterm lambs. J Appl Physiol (1985). 2012;112(3):481-489. doi:10.1152/japplphysiol.00995.2011
13. Normann E, Lacaze-Masmonteil T, Eaton F, Schwendimann L, Gressens P, Thébaud B. A novel mouse model of Ureaplasma-induced perinatal inflammation: effects on lung and brain injury. Pediatr Res. 2009;65(4):430-436. doi:10.1203/PDR.0b013e31819984ce
14. Hagberg H, Mallard C, Jacobsson B. Role of cytokines in preterm labour and brain injury. BJOG. 2005;112 Suppl 1:16-18. doi:10.1111/j.1471-0528.2005.00578.x
15. Ophelders DR, Gussenhoven R, Lammens M, et al. Neuroinflammation and structural injury of the fetal ovine brain following intra-amniotic Candida albicans exposure. J Neuroinflammation. 2016;13:29. Published 2016 Feb 2. doi:10.1186/s12974-016-0492-z
16. Saito M, Matsuda T, Okuyama K, et al. Effect of intrauterine inflammation on fetal cerebral hemodynamics and white-matter injury in chronically instrumented fetal sheep. Am J Obstet Gynecol. 2009;200(6):. doi:10.1016/j.ajog.2009.01.006
17. Paladini D, Malinger G, Birnbaum R, Monteagudo A, Pilu G, Salomon LJ, Timor-Tritsch IE. ISUOG Practice Guidelines (updated): sonographic examination of the fetal central nervous system. Part 2: performance of targeted neurosonography. Ultrasound Obstet Gynecol. 2021 Apr;57(4):661-671. doi: 10.1002/uog.23616. Epub 2021 Mar 18. Erratum in: Ultrasound Obstet Gynecol. 2022 Oct;60(4):591.
18. Paules C, Miranda J, Policiano C, Crovetto F, Youssef L, Hahner N, Nakaki A, Crispi F, Gratacós E, Eixarch E. Fetal neurosonography detects differences in cortical

development and corpus callosum in late-onset small fetuses. Ultrasound Obstet Gynecol. 2021 Jul;58(1):42-47.

19. Hagmann CF, Robertson NJ, Leung WC, Chong KW, Chitty LS. Foetal brain imaging: ultrasound or MRI. A comparison between magnetic resonance imaging and a dedicated multidisciplinary neurosonographic opinion. Acta Paediatr. 2008 Apr;97(4):414-9. doi: 10.1111/j.1651-2227.2008.00689.x. PMID: 18363950.
20. Higgins RD, Saade G, Polin RA, et al. Evaluation and Management of Women and Newborns With a Maternal Diagnosis of Chorioamnionitis: Summary of a Workshop. Obstet Gynecol. 2016;127(3):426-436. doi:10.1097/AOG.0000000000001246
21. F. Crispi, E. Llurba, C. Pedrero, E. Carreras, T. Higueras, E. Hermosilla, et al. Curvas de normalidad de la longitud cervical ecográfica según edad gestacional en población española. Prog Obstet Ginecol, 47 (2004), pp. 264-271
22. Cobo T, Palacio M, Martínez-Terrón M, et al. Clinical and inflammatory markers in amniotic fluid as predictors of adverse outcomes in preterm premature rupture of membranes. Am J Obstet Gynecol. 2011;205(2):126.e1-126.e1268. doi:10.1016/j.ajog.2011.03.050
23. Cobo T, Palacio M, Navarro-Sastre A, et al. Predictive value of combined amniotic fluid proteomic biomarkers and interleukin-6 in preterm labor with intact membranes. Am J Obstet Gynecol. 2009;200(5):499.e1-499.e4996. doi:10.1016/j.ajog.2008.12.036
24. Hadlock FP, Shah YP, Kanon DJ, Lindsey JV. Fetal crown-rump length: reevaluation of relation to menstrual age (5-18 weeks) with high-resolution real-time US. Radiology. 1992;182(2):501-505. doi:10.1148/radiology.182.2.1732970
25. Hadlock FP, Harrist RB, Carpenter RJ, Deter RL, Park SK. Sonographic estimation of fetal weight. The value of femur length in addition to head and abdomen measurements. Radiology 1984; 150: 535–40.
26. Malinger G, Paladini D, Haratz KK, Monteagudo A, Pilu GL, Timor-Tritsch IE. ISUOG Practice Guidelines (updated): sonographic examination of the fetal central nervous system. Part 1: performance of screening examination and indications for targeted

neurosonography. Ultrasound Obstet Gynecol. 2020 Sep;56(3):476-484. doi: 10.1002/uog.22145. Erratum in: Ultrasound Obstet Gynecol. 2022 Oct;60(4):591.

27. Medicinafetalbarcelona. Neurosonografía fetal. [medicinafetalbarcelona website]. https://medicinafetalbarcelona.org/protocolos/es/patologia-fetal/Neurosonografia_fetal.html. Accessed October, 2022
28. Chavez MR, Ananth CV, Smulian JC, Yeo L, Oyelese Y, Vintzileos AM. Fetal transcerebellar diameter measurement with particular emphasis in the third trimester: a reliable predictor of gestational age. Am J Obstet Gynecol. 2004 Sep;191(3):979-84.
29. Shimon Ginath, Tally Lerman-Sagie, Karina Haratz Krajden, Dorit Lev, Bina Cohen-Sacher, Jacob Bar & Gustavo Malinger (2013) The Fetal vermis, pons and brainstem: normal longitudinal development as shown by dedicated neurosonography, The Journal of Maternal-Fetal & Neonatal Medicine, 26:8, 757-762
30. Paules C, Miranda J, Policiano C, Crovetto F, Youssef L, Hahner N, Nakaki A, Crispi F, Gratacós E, Eixarch E. Fetal neurosonography detects differences in cortical development and corpus callosum in late-onset small fetuses. Ultrasound Obstet Gynecol. 2021 Jul;58(1):42-47.
31. Napolitano R, Molloholli M, Donadono V, Ohuma EO, Wanyonyi SZ, Kemp B, Yaqub MK, Ash S, Barros FC, Carvalho M, Jaffer YA, Noble JA, Oberto M, Purwar M, Pang R, Cheikh Ismail L, Lambert A, Gravett MG, Salomon LJ, Bhutta ZA, Kennedy SH, Villar J, Papageorghiou AT; International Fetal and Newborn Growth Consortium for the 21st Century (INTERGROWTH-21st). International standards for fetal brain structures based on serial ultrasound measurements from Fetal Growth Longitudinal Study of INTERGROWTH-21stProject. Ultrasound Obstet Gynecol. 2020 Sep;56(3):359-370.
32. Viñals F, Correa F, Gonçalves-Pereira PM. Anterior and posterior complexes: a step towards improving neurosonographic screening of midline and cortical anomalies. Ultrasound Obstet Gynecol. 2015 Nov;46(5):585-94.
33. Sari A, Ahmetoglu A, Dinc H, Saglam A, Kurtoglu U, Kandemir S, Gümele HR. Fetal biometry: size and configuration of the third ventricle. Acta Radiol. 2005 Oct;46(6):631-5.

34. Leibovitz Z, Shkolnik C, Haratz KK, Malinger G, Shapiro I, Lerman-Sagie T. Assessment of fetal midbrain and hindbrain in mid-sagittal cranial plane by three-dimensional multiplanar sonography. Part 1: comparison of new and established nomograms. Ultrasound Obstet Gynecol. 2014 Nov;44(5):575-80.
35. Falco P, Gabrielli S, Visentin A, Perolo A, Pilu G, Bovicelli L. Transabdominal sonography of the cavum septum pellucidum in normal fetuses in the second and third trimesters of pregnancy. Ultrasound Obstet Gynecol. 2000 Nov;16(6):549-53.
36. Malinger G, Lerman-Sagie T, Achiron R, Lipitz S. The subarachnoid space: normal fetal development as demonstrated by transvaginal ultrasound. Prenat Diagn. 2000 Nov;20(11):890-3.
37. Alonso I, Borenstein M, Grant G, Narbona I, Azumendi G. Depth of brain fissures in normal fetuses by prenatal ultrasound between 19 and 30weeks of gestation. Ultrasound Obstet Gynecol 2010; 36: 693–699.
38. Hahner N, Puerto B, Perez-Cruz M, Policiano C, Monterde E, Crispi F, Gratac ´ os E, Eixarch E. Altered cortical development in fetuses with isolated nonsevere ventriculomegaly assessed by neurosonography. Prenat Diagn 2018; 38:365–375.
39. Pistorius LR, Stoutenbeek P, Groenendaal F, de Vries L, Manten G, Mulder E, Visser G. Grade and symmetry of normal fetal cortical development: a longitudinal two- and three-dimensional ultrasound study. Ultrasound Obstet Gynecol 2010; 36: 700–708.
40. Achiron R, Achiron A. Development of the human fetal corpus callosum: a high-resolution, cross-sectional sonographic study. Ultrasound Obstet Gynecol. 2001 Oct;18(4):343-7.
41. Bonet-carne E, Dominguez M, Montede E, Pérez Cruz M, Eixarch E. Corpus callosum length and area measurements, an open source software for ultrasound and MR images. Virtual poster Nº 1934. In: Organization for human Brain Mapping (OHBM) Annual Meeting.
42. Witelson SF. The brain connection: the corpus callosum is larger in left-handers. Science. 1985; 229:665–668.
43. Cobo T, Burgos-Artizzu XP, Collado MC, et al. Noninvasive prediction models of intra-amniotic infection in women with preterm labor [published online ahead of print, 2022

722 Jul 20]. Am J Obstet Gynecol. 2022;S0002-9378(22)00581-6.
723 doi:10.1016/j.ajog.2022.07.027
724 44. Cobo T, Aldecoa V, Figueras F, et al. Development and validation of a multivariable
725 prediction model of spontaneous preterm delivery and microbial invasion of the amniotic
726 cavity in women with preterm labor. Am J Obstet Gynecol. 2020;223(3):421.e1-
727 421.e14. doi:10.1016/j.ajog.2020.02.049
728 45. Limperopoulos C, Soul JS, Gauvreau K, Huppi PS, Warfield SK, Bassan H, Robertson
729 RL, Volpe JJ, du Plessis AJ: Late gestation cerebellar growth is rapid and impeded by
730 pre- mature birth. Pediatrics 2005;115:688–695
731 46. Welsh JP, Yuen G, Placantonakis DG, Vu TQ, 22 Haiss F, O'Hearn E, Molliver ME,
732 Aicher SA: Why do Purkinje cells die so easily after global brain ischemia? Aldolase C,
733 EAAT4, and the cerebellar contribution to posthy-poxic myoclonus. Adv Neurol
734 2002;89:331–359.
735 47. Pierrat V, Marchand-Martin L, Arnaud C, et al. Neurodevelopmental outcome at 2 years
736 for preterm children born at 22 to 34 weeks' gestation in France in 2011: EPIPAGE-2
737 cohort study. BMJ. 2017;358:j3448. Published 2017 Aug 16. doi:10.1136/bmj.j3448
738 48. Bodensteiner JB, Johnsen SD: Cerebellar injury in the extremely premature infant:
739 newly recognized but relatively common outcome. J Child Neurol 2005;20:139–142.
740 49. Allin M, Matsumoto H, Santhouse AM, Nosarti C, AlAsady MH, Stewart AL, Rifkin L,
741 Murray RM: Cognitive and motor function and the size of the cerebellum in adolescents
742 born very pre-term. Brain 2001;124: 60–66.
743 50. Dubois J, Lefèvre J, Angleys H, et al. The dynamics of cortical folding waves and
744 prematurity-related deviations revealed by spatial and spectral analysis of
745 gyrification. Neuroimage. 2019;185:934-946. doi:10.1016/j.neuroimage.2018.03.005
746 51. Shimony JS, Smyser CD, Wideman G, et al. Comparison of cortical folding measures
747 for evaluation of developing human brain. Neuroimage. 2016;125:780-790.
748 doi:10.1016/j.neuroimage.2015.11.001
749 52. Dean JM, van de Looij Y, Sizonenko SV, Lodygensky GA, Lazeyras F, Bolouri H,
750 Kjellmer I, Huppi PS, Hagberg H, Mallard C. Delayed cortical impairment following

lipopolysaccharide exposure in preterm fetal sheep. Ann Neurol. 2011 Nov;70(5):846-56. doi: 10.1002/ana.22480. Epub 2011 Oct 14. PMID: 22002627

53. Egana-Ugrinovic G, Sanz-Cortes M, Figueras F, Couve-Perez C, Gratacos E. Fetal MRI insular cortical morphometry and its association with neurobehavior in late-onset small-for-gestational-age fetuses. Ultrasound Obstet Gynecol 2014; 44:322–329.
54. Gasquoine PG. Contributions of the insula to cognition and emotion. Neuropsychol Rev. 2014;24(2):77-87. doi:10.1007/s11065-014-9246-9
55. Craig AD. Significance of the insula for the evolution of human awareness of feelings from the body. Ann N Y Acad Sci. 2011;1225:72-82. doi:10.1111/j.1749-6632.2011.05990.x
56. De León Reyes NS, Bragg-Gonzalo L, Nieto M. Development and plasticity of the corpus callosum. Development. 2020 Sep 28;147(18):dev189738. doi: 10.1242/dev.189738. PMID: 32988974:
57. Moses P, Courchesne E, Stiles J, Trauner D, Egañas B, Edwards E: Regional size reduction in the human corpus callosum following preand perinatal brain injury. Cereb Cortex 2000; 10: 1200–1210. .
58. Paul LK: Developmental malformation of the corpus callosum: a review of typical callosal development and examples of developmental disorders with callosal involvement. J Neurodev Disord 2011; 3: 3–27. .
59. van de Looij Y, Lodygensky GA, Dean J, Lazeyras F, Hagberg H, Kjellmer I, Mallard C, Hüppi PS, Sizonenko SV. High-field diffusion tensor imaging characterization of cerebral white matter injury in lipopolysaccharide-exposed fetal sheep. Pediatr Res. 2012 Sep;72(3):285-92. doi: 10.1038/pr.2012.72. Epub 2012 Jun 5. PMID: 22907562.
60. Nosarti C, Rushe TM, Woodruff PWR, Stewart AL, Rifkin L, Murray RM. Corpus callosum size and very preterm birth: Relationship to neuropsychological outcome. Brain 2004; 127: 2080–2089.
61. Liu F, Cao S, Liu J, Du Z, Guo Z, Ren C. Ultrasound measurement of the corpus callosum and neural development of premature infants. Neural Regen Res. 2013;8(26):2432-2440. doi:10.3969/j.issn.1673-5374.2013.26.004

62. Rothermundt M, Ponath G, Arolt V. S100B in schizophrenic psychosis. Int Rev Neurobiol. 2004;59:445-470. doi:10.1016/S0074-7742(04)59017-7
63. Nagdyman N, Kömen W, Ko HK, Müller C, Obladen M. Early biochemical indicators of hypoxic-ischemic encephalopathy after birth asphyxia. Pediatr Res. 2001;49(4):502-506. doi:10.1203/00006450-200104000-00011
64. Gazzolo D, Bruschettini M, Lituania M, Serra G, Bonacci W, Michetti F. Increased urinary S100B protein as an early indicator of intraventricular hemorrhage in preterm infants: correlation with the grade of hemorrhage. Clin Chem. 2001;47(10):1836-1838.
65. Rosén H, Sunnerhagen KS, Herlitz J, Blomstrand C, Rosengren L. Serum levels of the brain-derived proteins S-100 and NSE predict long-term outcome after cardiac arrest. Resuscitation. 2001;49(2):183-191. doi:10.1016/s0300-9572(00)00348-8
66. Arca G, Arnaez J, Agut T, et al. Neuron-specific enolase is correlated with lesion topology, relative infarct volume and outcome of symptomatic NAIS. Arch Dis Child Fetal Neonatal Ed. 2020;105(2):132-137. doi:10.1136/archdischild-2018-316680
67. León-Lozano MZ, Arnaez J, Valls A, et al. Cerebrospinal fluid levels of neuron-specific enolase predict the severity of brain damage in newborns with neonatal hypoxic-ischemic encephalopathy treated with hypothermia. PLoS One. 2020;15(6):e0234082. Published 2020 Jun 1. doi:10.1371/journal.pone.0234082
68. Lopez J, Mikaelian I, Gonzalo P. Amniotic fluid glial fibrillary acidic protein (AF-GFAP), a biomarker of open neural tube defects. Prenat Diagn. 2013;33(10):990-995. doi:10.1002/pd.4181
69. Azzolini F, Gilio L, Pavone L, et al. Neuroinflammation Is Associated with GFAP and sTREM2 Levels in Multiple Sclerosis. Biomolecules. 2022;12(2):222. Published 2022 Jan 27. doi:10.3390/biom12020222
70. Elimian A, Figueroa R, Patel K, Visintainer P, Sehgal PB, Tejani N. Reference values of amniotic fluid neuron-specific enolase. J Matern Fetal Med. 2001;10(3):155-158. doi:10.1080/714904324

71. Paules C, Miranda J, Policiano C, et al. Fetal neurosonography detects differences in cortical development and corpus callosum in late-onset small fetuses. Ultrasound Obstet Gynecol. 2021;58(1):42-47. doi:10.1002/uog.23592
72. Basso A, Youssef L, Nakaki A, et al. Fetal neurosonography at 31-35 weeks reveals altered cortical development in pre-eclampsia with and without small-for-gestational-age fetus. Ultrasound Obstet Gynecol. 2022;59(6):737-746. doi:10.1002/uog.24853
73. Pérez-Cruz M, Gómez O, Gibert M, Masoller N, Marimon E, Lip-Sosa D, Bennasar M, Bonet-Carne E, Gómez-Roig MD, Martínez-Crespo JM, Gratacós E, Eixarch E. Corpus callosum size by neurosonography in fetuses with congenital heart defect and relationship with expected pattern of brain oxygen supply. Ultrasound Obstet Gynecol. 2022 Feb;59(2):220-225. doi: 10.1002/uog.23684. Epub 2022 Jan 12. PMID: 33998077
74. Malinger G, Birnbam R, Haratz KK. Dedicated neurosonography for recognition of pathology associated with mild-to-moderate ventriculomegaly. Ultrasound Obstet Gynecol. 2020;56(3):319-323. doi:10.1002/uog.22155
75. Boutet ML, Eixarch E, Ahumada-Droguett P, et al. Fetal neurosonography and infant neurobehavior following conception by assisted reproductive technology with fresh or frozen embryo transfer. Ultrasound Obstet Gynecol. 2022;60(5):646-656. doi:10.1002/uog.24920
76. Chaemsaithong P, Romero R, Docheva N, et al. Comparison of rapid MMP-8 and interleukin-6 point-of-care tests to identify intra-amniotic inflammation/infection and impending preterm delivery in patients with preterm labor and intact membranes. J Matern Fetal Neonatal Med. 2018;31(2):228-244. doi:10.1080/14767058.2017.1281904
77. Nien JK, Yoon BH, Espinoza J, et al. A rapid MMP-8 bedside test for the detection of intra-amniotic inflammation identifies patients at risk for imminent preterm delivery. Am J Obstet Gynecol. 2006;195(4):1025-1030. doi:10.1016/j.ajog.2006.06.054

AUTHOR CONTRIBUTIONS:

CM, EE, TC, MP EG contributed to the concept.

CM, EE, TC, MP EG contributed to the study design.

CM, CR, ML, DB, LG, JP, EM, VA, AH, SF and TC contributed to the inclusion of participants and data collection.

CM, EE, VA, MP, EG, TC Contributed to data analysis and interpretation.

All authors contributed to the drafting and critical revision of the manuscript.

TABLE 1

Baseline, fetal and perinatal characteristics of the study population

Variables	Group 1: Intra-amniotic inflammation (n= 41)	Group 2: Non-intra-amniotic inflammation (n=54)	Group 3: Control (n=48)	p1 *(1 vs. 2)*	p2 *(1 vs. 3)*	p3 *(2 vs. 3)*
Maternal age (years)	33.5 (30.2-37.5)	33.1 (28.8-34.9)	33.6 (30.3-36.9)	0.15	0.63	0.08
Body mass index (Kg/m^2)	23.0 (20.2-27.8)	22.5 (20.3-26.8)	21.8 (20.8-27.1)	0.90	0.78	0.67
Race						
Caucasian, n (%)	29/38 (76.3)	37/50 (74.0)	41 (85.4)	0.36	0.34	0.11
Maghrebi, n (%)	3/38 (7.9)	0 (0)	1 (2.1)			
Hispanic, n (%)	4/38 (10.5)	6/50 (12.0)	6 (12.5)			
Asian, n (%)	1/38 (2.6)	4/50 (8.0)	0 (0)			
Other, n (%)	1/38 (2.6)	3/50 (6.0)	0 (0)			
Maternal smoking, n (%)	2/39 (5.1)	7 (13.0)	5/47 (10.6)	0.30	0.45	0.72
Nulliparity, n (%)	19 (46.3)	34/52 (65.4)	27 (56.3)	0.07	0.35	0.35
Assisted reproductive technique, n (%)	3/34 (8.8)	4/46 (8.7)	6/48 (12.5)	1.00	0.73	0.74
Preterm labor at admission (n 61)	13/61 (21)	48/61 (79)	-	<0.001		
Preterm prelabor rupture of membranes at admission *(n 34)*	28/34 (82)	6/34 (18)	-	<0.001		
Gestational age at amniocentesis (weeks)	28.9 (26.0-3)	27.7 (26.0-30.7)	29.4 (27.0-	0.37	0.26	0.71

			30.9)			
Days from inclusion to delivery	11 (6-17)	57 (33-74)	72 (59-81)	<0.001	<0.001	<0.001
Neonatal male sex, n (%)	26 (63.4)	32 (59.3)	22 (45.8)	0.68	0.10	0.18
Gestational age at delivery (weeks)	31.1 (27.7-32.4)	37.4 (34.3-39.3)	39.6 (38.9-40.3)	<0.001	<0.001	<0.001
Birthweight (g)	1557 (1080-2166)	2600 (2010-3110)	3270 (3000-3510)	<0.001	<0.001	<0.001
Birthweight centile	20.5 (5.5 - 47)	32 (9 - 59)	48 (19 - 76)	0.30	0.002	0.04
Clinical chorioamnionitis at delivery	7 (17.1)	3 (5.6)	0 (0)	0.12	0.004	0.09
Histological funisitis or chorioamnionitis						
Acute chorioamnionitis without funisitis, n (%)	12 (29.3)	4/26 (15.4)	1/20 (5)	0.02	<0.001	0.17
Acute chorioamnionitis with funisitis, n (%)	19 (46.3)	7/26 (26.9)	2/20 (10)			
Cesarean, n (%)	18 (43.9)	10 (18.5)	11 (22.9)	0.02	0.04	0.81
Induction of labor, n (%)	7 (17.1)	9 (16.7)	27 (56.3)	0.84	<0.001	<0.001
Non cephalic presentation, n (%)	14 (34.1)	3 (5.6)	3 (6.3)	0.001	1.00	0.001
Apgar <7 at 5 min, n (%)	3/37 (8.1)	0/43 (0)	0/45 (0)	0.10	0.09	NA
pH umbilical artery	7.27 (7.18-7.34)	7.24 (7.19-7.30)	7.21 (7.15-7.27)	0.38	0.12	0.55
Neonatal intensive care unit	26/38 (68.4)	11/45 (24.4)	0/46 (0)	<0.001	<0.001	<0.001

admission n (%) Major neonatal morbidity[1] or mortality, n (%)	14/38 (36.8)	3/45 (6.7)	0/46 (0)	0.001	<0.001	0.08

Data are presented as number (percentage) for qualitative variables or median (25th centile; 75th centile) for quantitative variables.

[1]Major complications defined by the presence of bronchopulmonary dysplasia, necrotizing enterocolitis, intraventricular hemorrhage, periventricular leukomalacia, retinopathy or early onset sepsis.

TABLE 2

Clinical, ultrasound and biochemical comparison according to the presence of intra-amniotic infection and/or inflammation in women with preterm labor and preterm prelabor rupture of membranes

Variables	Group 1: Intra-amniotic inflammation n= 41)	Group 2: Non-intra-amniotic inflammation (n=54)	p
Preterm prelabor rupture membranes at admission, n (%)	28 (68.3)	6 (11.1)	<0.001
C-reactive protein (mg/L)	1.06 (0.56-2.2)	0.51 (0.28-1.06)	0.02
White cell count (x10^9 / L)	11300 (8670-14490)	11235 (9470-13900)	0.39
Neutrophils (%)	81 (74-89)	78 (73-84)	0.76
Cervical length (mm)	20.5 (12.0-31.5)	13 (10-18)	<0.001
Amniotic fluid glucose (mg/dL)	22 (11-35)	41 (31-52)	<0.001
Amniotic fluid interleukin-6 (pg/mL)	32090 (7111.3-73038.3)	1171.5 (728.5-1918.8)	<0.001
Positive amniotic fluid culture, n (%)	19 (46.3%)	0 (0)	<0.001
Latency from admission to ultrasound (days)	2 (1-3)	2 (1-2)	0.07

Data are presented as number (percentage) for qualitative variables or median (25^{th} centile; 75^{th} centile) for quantitative variables.

TABLE 3

Fetal ultrasonographic comparison: fetal-placental and intracranial structures, cephalic biometrics

Variables	*Group 1: Intra-amniotic inflammation (n= 41)*	*Group 2: Non-intra-amniotic inflammation (n=54)*	*Group 3: Control (n=48)*	*p1 (1 vs. 2)*	*p2 (1 vs. 3)*	*p3 (2 vs. 3)*	*p4 (linearity trend among the three groups)*
Fetal-placental parameters							
Gestational age at ultrasound (weeks)	*27.9 (28.7-31-1)*	*29.6 (27-31.2)*	*29.4 (26.6-31.3)*	*0.38*	*0.48*	*0.90*	*0.46*
Estimated fetal weight at ultrasound (gr)	*1150 (864-1547)*	*1362.5 (1066.5-1741.5)*	*1380.5 (1088 - 1705)*	*0.14*	*0.12*	*0.87*	*0.09*
Estimated fetal weigth centile	*23 (9.5 – 60.5)*	*53.5 (22.5 – 70)*	*58.5 (27.5 – 75)*	*0.01*	*0.002*	*0.55*	*0.004*
Small for gestational age (estimated fetal weight< 10th centile)	*11 (26.8%)*	*7 (13.0%)*	*4 (8.3%)*	*0.09*	*0.02*	*0.45*	*0.02*
Umbilical artery pulsatility index	*0.92 (0.72-1.09)*	*0.99 (0.84-1.11)*	*1.03 (0.82-1.17)*	*0.21*	*0.17*	*0.60*	*0.08*
Middle cerebral artery pulsatility index	*1.82 (1.56-2.12)*	*1.76 (1.59-2.05)*	*2 (1.71-2.25)*	*0.17*	*0.89*	*0.14*	*0.30*
Ductus venosus pulsatility index	*0.41 (0.31-0.54)*	*0.46 (0.34-0.57)*	*1.93 (1.65-2.43)*	*0.21*	*0.11*	*0.80*	*0.24*
Uterine arteries pulsatility index average	*0.76 (0.63-0.96)*	*0.78 (0.64-0.95)*	*0.72 (0.64-0.89)*	*0.11*	*0.62*	*0.08*	*0.31*
Cephalic biometrics							
Biparietal diameter (mm)	*69.5 (62.5-75)*	*74 (68-78)*	*74 (68-79)*	*0.14*	*0.11*	*0.91*	*0.03*
Occipito-frontal diameter (mm)	*89 (82.5-98)*	*94 (87-100)*	*96.5 (89-102)*	*0.21*	*0.03*	*0.61*	*0.007*
Head circumference (mm)	*253 (235-276.5)*	*268 (248-287)*	*273.5 (248.5-288.5)*	*0.15*	*0.10*	*0.86*	*0.02*
Cephalic index (%)	*76.8*	*78.1*	*77.2*	*0.46*	*0.33*	*0.17*	*0.93*

	(73.8-79.1)	*(75.6-80.6)*	*(74.5-78.8)*				
Intracranial structures							
Transcerebellar diameter (mm)	*32.7 (29.8-37.6)*	*35.3 (31.2-39.6)*	*35.0 (31.3-38.3)*	*0.09*	*0.02*	*0.19*	*0.37*
Cerebellar vermis antero-posterior diameter (mm)	*14.6 (13.3-17.5)*	*15.05 (12.95-16.75)*	*15.4 (13.8-16.2)*	*0.13*	*0.81*	*0.20*	*0.89*
Cerebellar vermian height (mm)	*16.9 (15.5-19.6)*	*17.2 (16.0-18.9)*	*17.1 (15.7-19.0)*	*0.04*	*0.04*	*0.84*	*0.93*
Pontine antero-posterior diameter (mm)	*10.2 (9.3-11.3)*	*10.9 (9.8-11.9)*	*10.4 (9.6-11.8)*	*0.83*	*0.26*	*0.44*	*0.66*
Insular depth ratio[1]	*0.33 (0.32-0.34)*	*0.32 (0.31-0.34)*	*0.32 (0.30-0.32)*	*0.18*	*0.001*	*0.06*	*<0.001*
Right anterior horn of lateral ventricle (mm)	*1.7 (1.1-2)*	*1.7 (1.1-2)*	*1.5 (1.2-2)*	*0.68*	*0.99*	*0.85*	*0.57*
Left anterior horn of lateral ventricle (mm)	*1.65 (1.25-2.42)*	*1.6 (1.3-2.2)*	*1.5 (1.25-1.95)*	*0.94*	*0.67*	*0.46*	*0.33*
Right posterior horn of lateral ventricle (mm)	*4.6 (4-5.4)*	*5.05 (4.05-6.7)*	*4.5 (3.8-5.7)*	*0.09*	*0.21*	*0.58*	*0.91*
Left posterior horn of lateral ventricle (mm)	*4.75 (4-5.5)*	*5.1 (4.15-6.7)*	*4.45 (3.6-5.7)*	*0.28*	*0.92*	*0.30*	*0.50*
Third ventricle (mm)	*0.9 (0.6-1.3)*	*1.0 (0.8-1.2)*	*1.0 (0.8-1.2)*	*0.41*	*0.84*	*0.61*	*0.22*
Fourth ventricle height (mm)	*2.8 (2.4-3.6)*	*3.25 (2.6-4)*	*2.8 (2.4-3.1)*	*0.94*	*0.18*	*0.11*	*0.16*
Fourth ventricle width (mm)	*4 (2.8-4.5)*	*3.65 (3-4.1)*	*3.1 (2.6-3.5)*	*0.02*	*<0.001*	*0.04*	*0.004*
Cavum septum pellucidum width (mm)	*5.4 (4.6-6.6)*	*5.5 (4.6-6.3)*	*5.1 (4.8-5.9)*	*0.46*	*0.06*	*0.15*	*0.43*
Cisterna magna (mm)	*5.7 (4.9-6.8)*	*6.05 (5.2-7.1)*	*5.75 (5-6.65)*	*0.49*	*0.33*	*0.09*	*0.96*
Subarachnoid craniocortical width (mm)	*2.55 (2.2-3.2)*	*2.85 (2.3-3.45)*	*2.9 (2.6-3.3)*	*0.64*	*0.53*	*0.66*	*0.10*
Subarachnoid	*2 (1.4-2.5)*	*1.95 (1.5-2.5)*	*2.3 (1.8-*	*0.79*	*0.42*	*0.18*	*0.06*

sinocortical width (mm)		*2.6)*

Data are presented as number (percentage) for qualitative variables or median (25^{th} centile; 75^{th} centile) for quantitative variables.

Sample size for corpus callosum areas measurements were n=24 in the Intra-amniotic inflammation group; n=38 in the non-intra-amniotic inflammation group; and n=42 in the control group.

Statistical analysis adjusted for head circumference, centile, fetal sex, non-cephalic presentation and preterm prelabor rupture of membranes at admission. Occipito-frontal diameter was considered instead head circumference in the corpus callosum length adjustment.

[1] Depth ratios: Insular or sulcus depth (mm) / biparietal diameter (mm)

TABLE 4
Fetal ultrasonographic comparison: cortical development and corpus callosum

Variables	Group 1: Intra-amniotic inflammation (n= 41)	Group 2: Non-intra-amniotic inflammation (n=54)	Group 3: Control (n=48)	p1 *(1 vs. 2)*	p2 *(1 vs. 3)*	p3 *(2 vs. 3)*	p4 *(linearity trend among the three groups)*
Cortical development							
Sylvian fissure grading	4 (3-4)	4 (3-4)	4 (3-5)	0.78	0.10	0.14	0.07
Sylvian fissure depth ratio[1]	0.14 (0.12-0.16)	0.14 (0.13-0.16)	0.16 (0.15-0.17)	0.19	0.003	0.04	<0.001
Right parieto-occipital sulcus grading	3 (2-4)	3 (2-4)	3 (2-5)	0.54	0.15	0.38	0.16
Right parieto-occipital sulcus depth ratio[1]	0.09 (0.07-0.12)	0.11 (0.09-0.14)	0.11 (0.09-0.14)	0.06	0.01	0.82	0.05
Left parieto-occipital sulcus grading	3 (2-4)	3 (2-4)	3 (2-5)	0.93	0.25	0.39	0.35
Left parieto-occipital sulcus depth ratio[1]	0.10 (0.06-0.12)	0.11 (0.08-0.13)	0.11 (0.09-0.13)	0.69	0.18	0.39	0.06
Right cingulate sulcus grading	2 (1-4)	2.5 (2-4)	3 (1-4)	0.59	0.45	0.73	0.27
Right cingulate sulcus depth ratio[1]	0.03 (0.01-0.04)	0.04 (0.03-0.06)	0.04 (0.02-0.06)	0.03	0.09	0.42	0.10
Left cingulate sulcus grading	2 (1-4)	2.5 (2-4)	3 (1-4)	0.80	0.57	0.78	0.03
Left cingulate sulcus depth ratio[1]	0.03 (0.01-0.05)	0.04 (0.03-0.06)	0.04 (0.02-0.07)	0.21	0.31	0.38	0.21
Right calcarine sulcus grading	4 (2-5)	4 (3-5)	4 (2-5)	0.37	0.32	0.66	0.59
Right calcarine sulcus depth ratio[1]	0.13 (0.09-0.16)	0.14 (0.12-0.16)	0.14 (0.11-0.16)	0.14	0.55	0.28	0.54
Left calcarine sulcus grading	4 (2-5)	4 (3-5)	4 (2-5)	0.68	0.46	0.66	0.78
Left calcarine sulcus depth ratio[1]	0.13 (0.10-0.15)	0.14 (0.12-0.15)	0.13 (0.10-0.16)	0.59	0.93	0.45	0.82
Corpus callosum							
Corpus callosum	34.55	35.9	36.3	0.45	0.34	0.08	0.39

length (mm)	(31.6-37.1)	(33.15-39.6)	(33.5-38.3)				
Corpus callosum thickness (mm)	1.7 (1.5-1.9)	1.9 (1.55-2.15)	1.9 (1.6-2.1)	0.29	0.21	0.76	0.13
Corpus callosum total área (mm^2)	0.715 (0.587-0.810)	0.713 (0.630-0.819)	0.781 (0.713-0.912)	0.69	0.04	0.004	0.006
Witelson subregion 1 Rostrum (mm^2)	0.033 (0.018-0.042)	0.027 (0.015-0.036)	0.033 (0.022-0.050)	0.33	0.88	0.20	0.53
Witelson subregion 2 Genu (mm^2)	0.108 (0.078-0.131)	0.095 (0.071-0.094)	0.118 (0.094-0.143)	0.67	0.15	0.16	0.07
Witelson subregion 3 Rostral body (mm^2)	0.158 (0.126-0.169)	0.156 (0.136-0.175)	0.179 (0.147-0.203)	0.61	0.02	0.002	0.004
Witelson subregion 4 Anterior midbody (mm^2)	0.085 (0.063-0.098)	0.080 (0.072-0.094)	0.089 (0.078-0.103)	0.37	0.28	0.03	0.05
Witelson subregion 5 posterior midbody (mm^2)	0.074 (0.054-0.084)	0.076 (0.067-0.090)	0.088 (0.073-0.107)	0.61	0.02	0.02	0.002
Witelson subregion 6 isthmus (mm^2)	0.052 (0.046-0.066)	0.058 (0.047-0.076)	0.069 (0.058-0.088)	0.42	0.003	0.007	<0.001
Witelson subregion 7 Splenium (mm^2)	0.214 (0.170-0.234)	0.202 (0.172-0.241)	0.213 (0.181-0.249)	0.99	0.31	0.24	0.20

Data are presented as number (percentage) for qualitative variables or median (25^{th} centile; 75^{th} centile) for quantitative variables.

Sample size for corpus callosum areas measurements were n=24 in the Intra-amniotic inflammation group; n=38 in the non-intra-amniotic inflammation group; and n=42 in the control group.

Statistical analysis adjusted for head circumference, centile, fetal sex, non-cephalic presentation and preterm prelabor rupture of membranes at admission. Occipito-frontal diameter was considered instead head circumference in the corpus callosum length adjustment.

[1] Depth ratios: Insular or sulcus depth (mm) / biparietal diameter (mm)

933

934

935

TABLE 5

Evaluation of amniotic fluid biomarkers in the entire study group

Variables	Group 1: Intra-amniotic inflammation (n= 41)	Group 2: Non-intra-amniotic inflammation (n=54)	Control Samples (n=20)	p1 *(1 vs. 2)*	p2 *(1 vs. control)*	p3 *(2 vs. control)*	p4 *(linearity trend among the three groups)*
Gestational age at amniocentesis (weeks)	28.9 (26.0-3)	27.7 (26.0-30.7)	29.2 (28.2-33.3)	0.37	0.22	0.09	0.02
Estimated fetal weight at ultrasound (gr)	1150.0 (864.0-1547.0)	1362.5 (1066.5-1741.5)	1328.0 (1025.0-1991.0)	0.14	0.05	0.26	0.04
Neonatal male sex, n (%)	26 (63.4)	32 (59.3)	12 (60.0)	0.68	0.92	0.97	0.74
Estimated fetal weight centile	23.0 (9.5-60.5)	53.5 (22.5-70.0)	43.5 (22.5-63.0)	0.01	0.19	0.49	0.09
Neurospecific enolase (pg/ml)	11804.55 (6213.4-21098.75)	8397.7 (3682.1-17398.3)	2393.65 (1717.05-3209.25)	0.47[1]	0.001[2]	<0.001[2]	<0.001
Protein S100B (pg/ml)	2030.6 (993-4883.45)	1070.3 (365.1-1463.2)	74.8 (44.65-93.7)	0.038[1]	0.048[2]	<0.001[2]	<0.001
Glial fibrillary acidic protein (ng/ml)	1.01 (0.54-3.88)	0.965 (0.59-2.07)	0.24 (0.20-0.28)	0.95[1]	0.18[2]	0.15[2]	0.002
Detectable Glial fibrillary acidic protein[3], n (%)	68.29	62.96	30	0.59[1]	0.002[2]	0.005[2]	0.010

Data are presented as number (percentage) for qualitative variables or median (25th centile; 75th centile) for quantitative variables.

[1] Adjusted for centile, fetal sex and gestational age at amniocentesis and preterm prelabor rupture of membranes at admission.

[2] Adjusted for centile, fetal sex and gestational age at amniocentesis.

[3] Including only the sample levels of detectable glial fibrillary acidic protein.

936

937

Figure 1

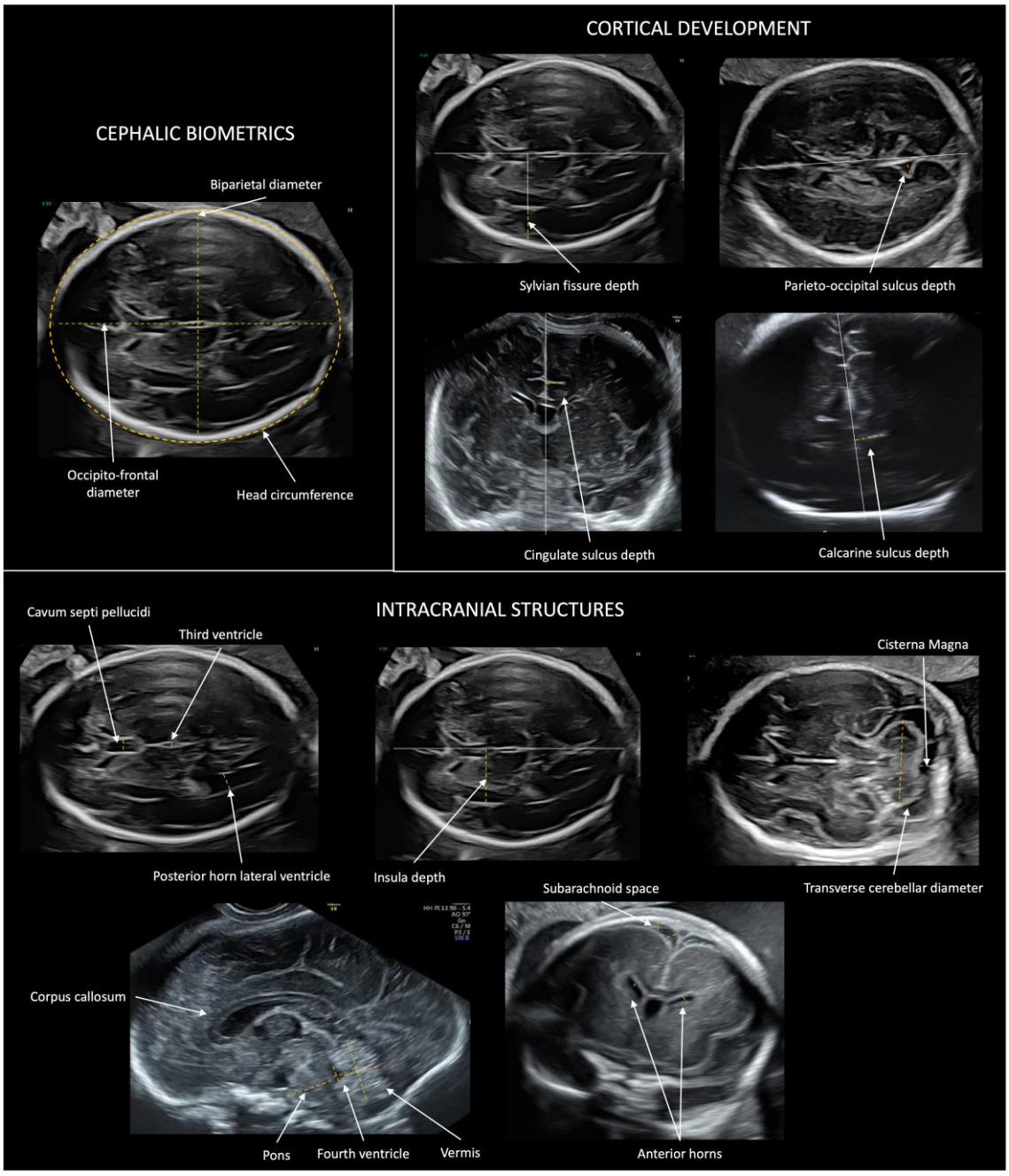
CEPHALIC BIOMETRICS
Biparietal diameter
Occipito-frontal diameter
Head circumference
CORTICAL DEVELOPMENT
Sylvian fissure depth
Parieto-occipital sulcus depth
Cingulate sulcus depth
Calcarine sulcus depth
INTRACRANIAL STRUCTURES
Cavum septi pellucidi
Third ventricle
Posterior horn lateral ventricle
Insula depth
Cisterna Magna
Transverse cerebellar diameter
Subarachnoid space
Corpus callosum
Pons
Fourth ventricle
Vermis
Anterior horns

946 Figure 2

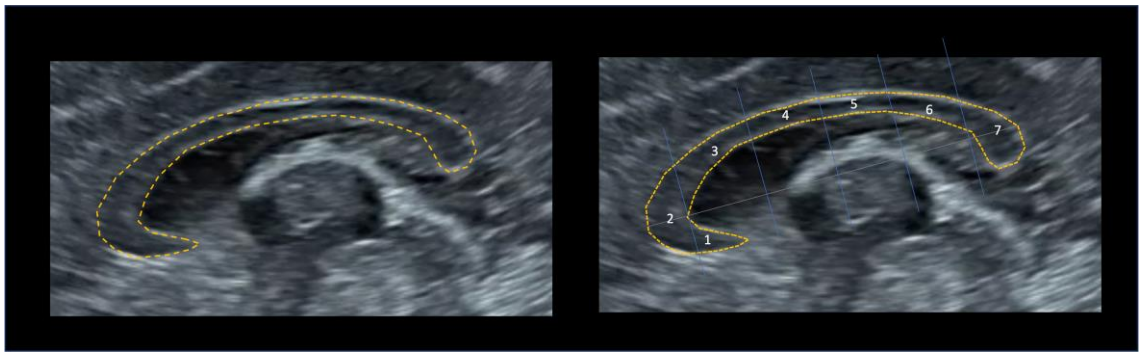

947

948

949 Figure 3

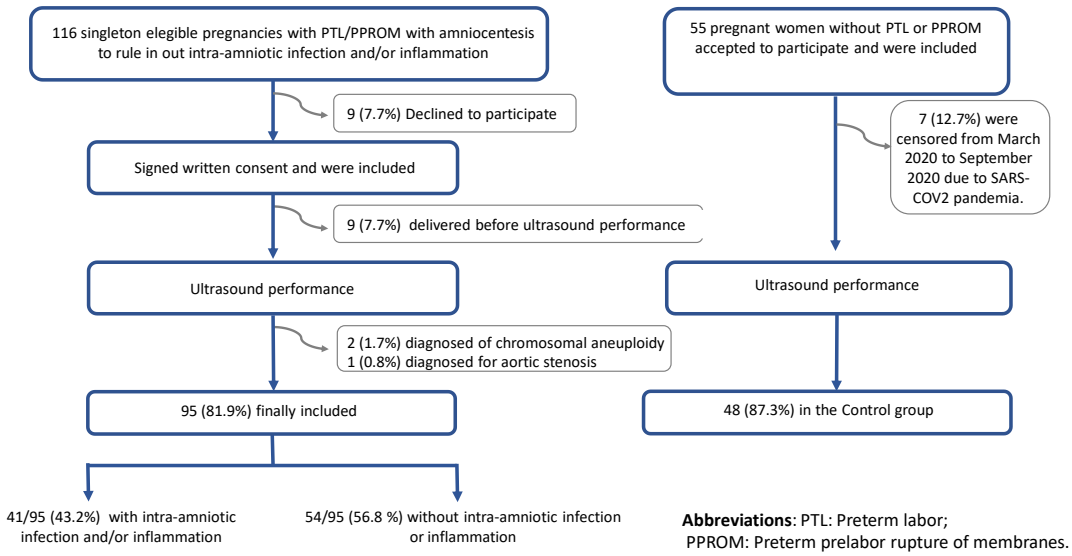

Abbreviations: PTL: Preterm labor;
PPROM: Preterm prelabor rupture of membranes.

950

951

952

953

954

955

956

957

958

Figure 4

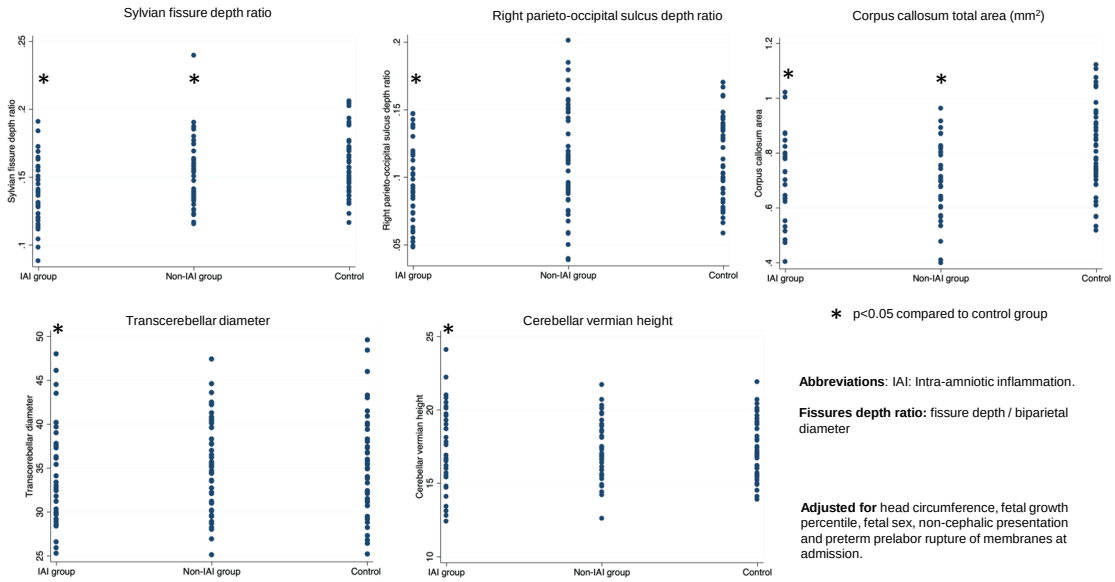

Abbreviations: IAI: Intra-amniotic inflammation.

Fissures depth ratio: fissure depth / biparietal diameter

Adjusted for head circumference, fetal growth percentile, fetal sex, non-cephalic presentation and preterm prelabor rupture of membranes at admission.

Figure 5

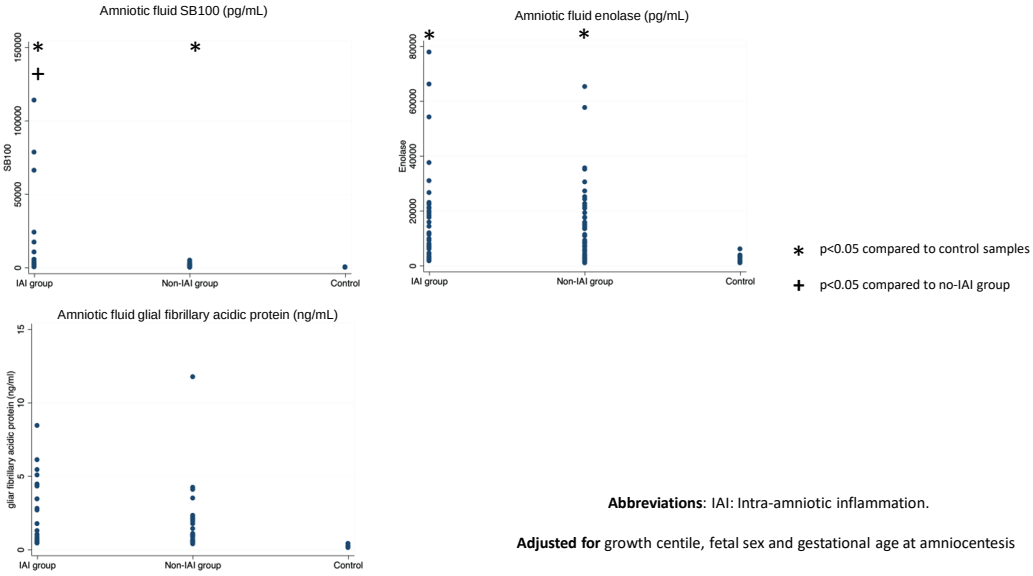

Abbreviations: IAI: Intra-amniotic inflammation.

Adjusted for growth centile, fetal sex and gestational age at amniocentesis

969 SUPPLEMENTARY TABLES

970

TABLE S1

Microorganisms isolated in the positive amniotic fluid cultures

Gestational age at amniocentesis (weeks)	Microorganism isolated in amniotic fluid
23.3	*Ureaplasma urealyticum*
30.9	*Peptoniphilus indoliticus*
26.1	*Capnocytophaga sputigena* and *fusobacterium* spp.
30.9	*Ureaplasma urealyticum*
32.4	*Ureaplasma urealyticum*
33.4	*Ureaplasma urealyticum*
26.1	*Fusobacterium nucleatum*
27.6	*Peptoniphilus harei*
25.4	*Fusobacterium nucleatum*
29.0	*Ureaplasma urealyticum*
23.9	*Ureaplasma urealyticum*
30.1	*Ureaplasma urealyticum* and *streptococcus mitis*
27.0	Extended spectrum beta-lactamase producing *Escherichia coli*
30.4	*Ureaplasma urealyticum*
27.4	*Ureaplasma urealyticum*
25.7	*Ureaplasma urealyticum*
26.9	*Escherichia coli* and *Bacteroides vulgatus*
29.9	*Peptoniphilus indolicus*
26.1	*Ureaplasma urealyticum*

971

972

TABLE S2

Indications for amniocentesis in non-exposed cohort

Gestational age at amniocentesis (weeks+days)	Indication for amniocentesis
25+0	Right renal agenesis
26+0	Aberrant left subclavian artery
26+3	Congenital talipes equinovarus
27+0	Aberrant right subclavian artery and congenital talipes equinovarus
28+0	Hyperechogenic fetal bowel
28+3	Moderate renal pyelectasis
28+4	Small for gestational age and long bones at -2 standard deviations.
28+5	Mild polyhydramnios + hyperechogenic fetal bowel
28+6	Mild renal pyelectasis
29+1	Small for gestational age
29+3	Hyperechogenic fetal bowel
29+6	Hyperechogenic fetal bowel
31+4	Hypospadias
32 +0	Aberrant right subclavian artery and 2mm muscular ventricular septal defect
33+0	Small for gestational age and muscular ventricular septal defect (2 mm)
33+6	Absent ductus venosus
35+1	Small for gestational age and muscular ventricular septal defect (2 mm)
35+3	Absent ductus venosus
36+1	Long bones at -1 to -2 standard deviations.
36+3	Long bones at -2 to -3 standard deviations.

All the amniocenteses were performed for extra-brain reasons, the pregnancies did not present risk factors for brain anomalies, and normal results in the amniotic fluid analysis (genetics and infections) and healthy offspring were confirmed in all cases.

Small for gestational age cases were all between the 3rd and 10th centile with a normal Doppler study.

973

974

TABLE S3

Baseline, fetal and perinatal characteristics according to the presence of intra-amniotic inflammation

Variables	Intra-amniotic infection (n= 19)	Sterile intra-amniotic inflammation (n= 22)	*p*
Maternal and fetal characteristics			
Maternal age (years)	33.8 (30.5-37.0)	33.7 (28.2-37.6)	0.39
Body mass index (Kg/m^2)	22.7 (20.0-28.3)	23.0 (21.1-25.8)	0.97
Race			
Caucasian, n (%)	12/17 (70.1%)	17/21 (81%)	0.56
Maghrebi, n (%)	2/17 (11.8%)	1/21 (4.8%)	
Hispanic, n (%)	1/17 (5.9%)	3/21 (14.3%)	
Asian, n (%)	1/17 (5.9%)	0 (0)	
Other, n (%)	1/17 (5.9%)	0 (0)	
Maternal smoking, n (%)	0 (0)	2/39 (5.1%)	0.49
Primiparity, n (%)	6 (33.3%)	13 (59.1%)	0.11
Assisted reproductive technique, n (%)	1/15 (6.7%)	2/19 (10.5%)	1.00
Gestational age at inclusion (weeks)	27.6(26.0-30.4)	28.9 (26.0-3)	0.52
Days from inclusion to delivery (days)	9 (5-16)	13 (6-23)	0.20
Perinatal data			
Neonatal male sex, n (%)	11 (61.1%)	15 (68.2%)	0.64
Gestational age at delivery (weeks)	30.3 (27.4-32.1)	31.4 (28.3-33.0)	0.19
Birthweight (g)	1300 (1040-1600)	1748 (1282-2240)	0.03
Birthweight centile	11.5 (3-21)	29.5 (6-51)	0.33
Clinical chorioamnionitis at delivery	4 (21.1)	3 (13.6)	0.69
Histological funisitis or chorioamnionitis			
Acute chorioamnionitis without funisitis, n (%)	8 (42.1)	4 (18.2)	0.24

Acute chorioamnionitis + funisitis, n (%)	7 (36.8)	12 (54.6)	
Cesarean, n (%)	12 (63.2)	6 (27.3)	0.02
Induction of labor, n (%)	4 (21.1)	3 (13.6)	0.69
Non cephalic presentation, n (%)	9 (47.4)	5 (22.7)	0.10
Apgar <7 at 5 min, n (%)	1/18 (5.6)	2/19 (10.5)	1.00
pH umbilical artery	7.26 (7.08-7.35)	7.27 (7.18-7.34)	0.30
Neonatal intensive care unit admission n (%)	13/18 (72.2)	13/20 (65.0)	0.63
Major neonatal morbidity[1] or mortality, n (%)	6/18 (33.3)	8/20 (40.0)	0.67

Data are presented as number (percentage) for qualitative variables or median (25th centile; 75th centile) for quantitative variables.

[1] Major complications defined by the presence of bronchopulmonary dysplasia, necrotizing enterocolitis, intraventricular hemorrhage, periventricular leukomalacia, retinopathy or early onset sepsis.

975

976

977

TABLE S4

Clinical, ultrasound and biochemical comparison according to the presence of intra-amniotic inflammation

Variables	Intra-amniotic infection (n= 19)	Sterile intra-amniotic inflammation (n= 22)	*p*
Preterm prelabor rupture of membranes at admission, n (%)	13 (68.4)	15 (68.2)	0.78
C-reactive protein (mg/L)	1.71 (1.22-3.1)	0.59 (0.23-1.01)	<0.001
White cell count ($x10^9$ / L)	13915 (8720-17950)	11250 (8660 – 13280)	0.37
Neutrophils (%)	83 (80-89)	77 (73-88)	0.14
Cervical length (mm)	20 (16-30)	21 (10-31)	0.78
Amniotic fluid glucose (mg/dL)	20.5 (3-32)	25.5 (10-38)	<0.001
Amniotic fluid interleukin-6 (pg/mL)	67994.45 (37593.2 – 143387.0)	17600.4 (4282.1-33581.8)	<0.001
Positive amniotic fluid culture, n (%)	19 (100%)	0 (0)	<0.001
Latency from admission to ultrasound (days)	1.5 (1-3)	2 (1-3)	0.06

Data are presented as number (percentage) for qualitative variables or median (25^{th} centile; 75^{th} centile) for quantitative variables.

978

979

980

TABLE S5

Ultrasound fetal brain parameters in patients with intra-amniotic inflammation

Variables	Intra-amniotic infection (n= 19)	Sterile intra-amniotic inflammation (n= 22)	*p*
Fetal-placental parameters			
Gestational age at ultrasound (weeks)	27.6 (26.3 – 30.6)	29.2 (26.3- 31.7)	0.41
Estimated fetal weight at ultrasound (gr)	980 (857 – 1508)	1230 (966 – 1712)	0.37
Estimated fetal weight centile	20 (10-43)	26 (7-64)	0.83
Small for gestational age (estimated fetal weight< 10th centile)	5 (26.3%)	6 (27.3%)	0.97
Umbilical artery pulsatility index	0.81 (0.71-0.98)	0.93 (0.73-1.16)	0.12
Middle cerebral artery pulsatility index	1.81 (1.68-2.31)	1.82 (1.54-2.05)	0.22
Ductus venosus pulsatility index	0.41 (0.31-0.59)	0.39 (0.31-0.53)	0.59
Uterine arteries pulsatility index average	0.85 (0.63-1.10)	0.74 (0.63-0.845)	0.89
Cephalic biometrics			
Bieparietal diameter (mm)	66 (63-74)	71.5 (62-77)	0.61
Frontal-occipital diameter (mm)	87 (84-92)	94 (83-99)	0.35
Head circumference (mm)	246 (235-269)	264 (241-278)	0.51
Cephalic index (%)	76.3 (73.9-79.3)	76.8 (73.7-78.6)	0.53
Brain structures			
Transcerebellar diameter (mm)	32.7 (29.9-37.8)	33.4 (29.8 – 37.3)	0.26
Cerebellar vermis AP diameter (mm)	14.3 (12.9-18.3)	14.75 (13.9-16.9)	0.40
Cerebellar vermian height (mm)	16.6 (14.8-20.2)	17.35 (16.2-19.3)	0.42
Pons anterior-posterior diameter (mm)	19 (8.7-10.7)	10.8 (9.8-11.5)	0.26
Insular depth ratio[1]	0.33 (0.32-0.34)	0.34 (0.32-0.35)	0.39
Right anterior horn of lateral ventricle (mm)	1.8 (1.65-2.15)	1.6 (1.0-2.0)	0.20
Left anterior horn of lateral ventricle (mm)	1.9 (1.25-2.4)	1.55 (1.3-2.55)	0.73

Right posterior horn of lateral ventricle (mm)	5.05 (4.25-5.5)	4.3 (3.5-4.6)	0.09
Left posterior horn of lateral ventricle (mm)	5.05 (4.05-5.5)	4.6 (4.0-5.5)	0.66
Third ventricle (mm)	0.9 (0.75-1.2)	0.9 (0.5-1.4)	0.47
Fourth ventricle height (mm)	2.8 (2.5-3.4)	2.8 (2.4-3.6)	0.91
Fourth ventricle width (mm)	4.1 (2.8-4.4)	3.9 (3.3-4.8)	0.80
Cavum septum pellucidum width (mm)	5.4 (4.9-6.8)	5.4 (4.6-6.3)	0.35
Cisterna magna (mm)	5.8 (5.1-7.3)	5.2 (4.7-6.1)	0.04
Subarachnoid craniocortical width (mm)	2.5 (2.2-3.4)	2.55 (2.3-3.1)	0.41
Subarachnoid sinocortical width (mm)	2.0 (1.4-2.7)	1.85 (1.4-2.4)	0.11
Cortical development			
Sylvian fissure grading	3.5 (3-4)	3.5 (3-4)	0.70
Sylvian fissure depth ratio[1]	0.13 (0.12-0.15)	0.14 (0.13-0.16)	0.18
Right parieto-occipital sulcus grading	3 (2-4)	2 (2-4)	0.44
Right parieto-occipital sulcus depth ratio[1]	0.10 (0.06-0.12)	0.09 (0.07-0.12)	0.98
Left parieto-occipital sulcus grading	3 (2-4)	2 (2-4)	0.19
Left parieto-occipital sulcus depth ratio[1]	0.10 (0.06-0.11)	0.10 (0.08-0.12)	0.42
Right cingulate sulcus grading	1.5 (1-4)	2 (1-4)	0.91
Right cingulate sulcus depth ratio[1]	0.02 (0.10-0.03)	0.03 (0.02-0.04)	0.34
Left cingulate sulcus grading	1 (1-4)	2.5 (1-4)	0.62
Left cingulate sulcus depth ratio[1]	0.03 (0.01-0.04)	0.03 (0.01-0.07)	0.44
Right calcarine sulcus grading	4 (2-4)	4 (2.5-5)	0.79
Right calcarine sulcus depth ratio[1]	0.13 (0.09-0.14)	0.14 (0.08-0.16)	0.89
Left calcarine sulcus grading	4 (2-4)	4 (3-5)	0.55
Left calcarine sulcus depth ratio[1]	0.13 (0.10-0.17)	0.13 (0.11-015)	0.30
Corpus callosum			
Corpus callosum length (mm)	34.55 (31.65-37.0)	34.40 (31.6-37.1)	0.41
Corpus callosum thickness (mm)	1.6 (1.5-1.8)	1.75 (1.50-2.0)	0.45

Corpus callosum total área (mm^2) (n= 9/15)	0.634 (0.483-0.797)	0.730 (0.633-0.823)	0.87
Witelson subregion 1 (mm^2) (n= 9/15)	0.040 (0.026-0.042)	0.027 (0.017-0.042)	0.88
Witelson subregion 2 (mm^2) (n= 9/15)	0.110 (0.074-0.113)	0.107 (0.081-0.131)	0.94
Witelson subregion 3 (mm^2) (n= 9/15)	0.130 (0.101-0.170)	0.159 (0.156-0.169)	0.44
Witelson subregion 4 (mm^2) (n= 9/15)	0.066 (0.060-0.096)	0.085 (0.068-0.098)	0.38
Witelson subregion 5 (mm^2) (n= 9/15)	0.071 (0.051-0.090)	0.076 (0.056-0.084)	0.67
Witelson subregion 6 (mm^2) (n= 9/15)	0.048 (0.045-0.062)	0.054 (0.046-0.066)	0.63
Witelson subregion 7 (mm^2) (n= 9/15)	0.212 (0.115-0.236)	0.216 (1.177-0.231)	0.83

Data are presented as number (percentage) for qualitative variables or median (25^{th} centile; 75^{th} centile) for quantitative variables.

Results were adjusted for head circumference, centile, fetal sex and non-cephalic presentation. The adjustment for head circumference was not included in the cephalic biometrics, depth ratios and sulcus operculization. Occipito-frontal diameter was considered instead head circumference in the corpus callosum length adjustment.

[1] Depth ratios: Insular or sulcus depth (mm) / biparietal diameter (mm)

981

982

983

TABLE S6

Amniotic fluid biomarkers concentrations according to the presence of intra-amniotic inflammation

Variables	Intra-amniotic infection (n= 19)	Sterile intra-amniotic inflammation (n= 22)	*p*
Neuron-specific enolase (pg/ml)	15073.25 (9160.3-21230.6)	6983.45 (3946.4-20966.9)	0.61
Protein S100B (pg/ml)	3573.9 (1307.4-17158.3)	1657.8 (758.8-2533.2)	0.02
Glial fibrillary acidic protein (ng/ml)	1.39 (0.63-3.88)	0.82 (0.51-4.25)	0.53
Detectable glial fibrillary acidic protein (%)	63.16	72.73	0.51

Data are presented as number (percentage) for qualitative variables or median (25th centile; 75th centile) for quantitative variables. p was adjusted for centile, fetal sex, gestational age at amniocentesis and preterm prelabor rupture of membranes at admission.

[1]*Including only the sample levels of detectable g*lial fibrillary acidic protein.

TABLE S7

Ultrasound and amniotic fluid fetal brain biomarkers in patients delivered preterm or at term

Variables	Spontaneous preterm delivery < 37 weeks (n= 26)	At term (n 35)	*p*
Sylvian fissure depth ratio	0.15 (0.13-0.16)	0.14 (0.13-0.17)	0.34
Right parieto-occipital sulcus depth ratio	0.09 (0.07-0.13)	0.11 (0.09-0.13)	0.24
Corpus callosum total área (mm^2)	0.68 (0.53-0.78)	0.73 (0.64-0.82)	0.12
Transcerebellar diameter (mm)	33.4 (30.1-37.3)	35.4 (29.9-39.6)	0.40
Cerebellar vermian height (mm)	16.9 (15.9-18-5)	16.9 (15-9-18.6)	0.64
Neuron-specific enolase (pg/ml)	10805 (6371-17566)	6832 (2888-15823)	0.25
Protein S100B (pg/ml)	1645 (814-2497)	734 (280-1386)	0.001
Glial fibrillary acidic protein (ng/ml)	0.94 (0.5-2.8)	0.55 (0.3-1.08)	0.10

Data are presented as median (25^{th} centile; 75^{th} centile). p was adjusted for centile, fetal sex and gestational age at amniocentesis (in the amniotic fluid biomarkers) or gestational age at neurosonography and presentation (in the ultrasound structures).

1022

TABLE S8

Correlation between amniotic fluid IL-6 and brain structures and amniotic fluid biomarkers in preterm labor with intact membranes and preterm prelabor rupture of membranes groups

Brain structures	Pearson's correlation coefficient	p
Transcerebellar diameter (mm)	-0.25	0.02
Cerebellar vermian height (mm)	-0.16	0.16
Insular depth ratio[1]	0.03	0.75
Left Levene ventricular index (mm)	-0.10	0.46
Fourth ventricular width (mm)	-0.07	0.60
Sylvian fissure depth ratio[1]	-0.17	0.13
Right parieto-occipital sulcus depth ratio[1]	-0.28	0.01
Right cingulate sulcus depth ratio[1]	-0.25	0.04
Corpus callosum length (mm)	-0.19	0.10
Corpus callosum total área (mm^2)	-0.26	0.039
Witelson subregion 1 (mm^2)	0.10	0.43
Witelson subregion 2 (mm^2)	-0.16	0.22
Witelson subregion 3 (mm^2)	-0.25	0.048
Witelson subregion 4 (mm^2)	-0.16	0.22
Witelson subregion 5 (mm^2)	-0.22	0.09
Witelson subregion 6 (mm^2)	-0.25	0.048
Witelson subregion 7 (mm^2)	-0.30	0.019
Amniotic fluid Neuron-specific enolase (pg/ml)	0.86	0.019
Amniotic fluid protein S100B (pg/ml)	0.40	0.09
Amniotic fluid Glial fibrillary acidic protein (ng/ml)	0.93	0.01

[1] Depth ratios: Insular or sulcus depth (mm) / biparietal diameter (mm)

1023
1024